

This discussion paper is/has been under review for the journal *Climate of the Past* (CP). Please refer to the corresponding final paper in CP if available.

Millennial and sub-millennial scale climatic variations recorded in polar ice cores over the last glacial period

E. Capron¹, A. Landais¹, J. Chappellaz², A. Schilt³, D. Buiron², D. Dahl-Jensen⁴, S. J. Johnsen⁴, J. Jouzel¹, B. Lemieux-Dudon², L. Loulergue², M. Leuenberger³, V. Masson-Delmotte¹, H. Mayer⁵, H. Oerter⁵, and B. Stenni⁶

¹Institut Pierre-Simon Laplace/Laboratoire des Sciences du Climat et de l'Environnement, CEA-UMR INSU/CNRS 8212-UVSQ, 91191 Gif-sur-Yvette, France

²Laboratoire de Glaciologie et Géophysique de l'Environnement, CNRS-UJF, 38400 St Martin d'Hères, France

³Climate and Environmental Physics, Physics Institute, and Oeschger Centre for Climate Change Research, University of Bern, Sidlerstrasse 5, 3012 Bern, Switzerland

⁴Centre for Ice and Climate, Niels Bohr Institute, University of Copenhagen, Juliane Maries Vej 30, 2100, Copenhagen, Denmark

⁵Alfred Wegener Institute for Polar and Marine Research, P.O. Box 120161, 27515 Bremerhaven, Germany

Title Page

Abstract

Introduction

Conclusions

References

Tables

Figures

◀

▶

◀

▶

Back

Close

Full Screen / Esc

Printer-friendly Version

Interactive Discussion



⁶University of Trieste, Department of Geological, Environmental and Marine Sciences, Via E. Weiss 2, 34127 Trieste, Italy

Received: 13 January 2010 – Accepted: 18 January 2010 – Published: 11 February 2010

Correspondence to: E. Capron (emilie.capron@Isce.ipsl.fr)

CPD

6, 135–183, 2010

**Millennial and
sub-millennial scale
climatic variations**

E. Capron et al.

Title Page

Abstract

Introduction

Conclusions

References

Tables

Figures

⏪

⏩

◀

▶

Back

Close

Full Screen / Esc

Printer-friendly Version

Interactive Discussion



Abstract

Since its discovery in Greenland ice cores, the millennial scale climatic variability of the last glacial period has been increasingly documented at all latitudes with studies focusing mainly on Marine Isotopic Stage 3 (MIS 3; 28–60 thousand of years before present, hereafter ka) and characterized by short Dansgaard-Oeschger (DO) events. Recent and new results obtained on the EPICA and NorthGRIP ice cores now precisely describe the rapid variations of Antarctic and Greenland temperature during MIS 5 (73.5–123 ka), a time period corresponding to relatively high sea level. The results display a succession of long DO events enabling us to highlight a sub-millennial scale climatic variability depicted by i) short-lived and abrupt warming events preceding some Greenland InterStadial (GIS) (precursor-type events) and ii) abrupt warming events at the end of some GIS (rebound-type events). The occurrence of these secondary events is suggested to be driven by the Northern Hemisphere summertime insolation at 65° N together with the internal forcing of ice sheets. Thanks to a recent NorthGRIP-EPICA Dronning Maud Land (EDML) common timescale over MIS 5, the bipolar sequence of climatic events can be established at millennial to sub-millennial timescale. This provides evidence that a linear relationship is not satisfactory in explaining the link between Antarctic warming amplitudes and the duration of their concurrent Greenland Stadial (GS) for the entire glacial period. The conceptual model for a thermal bipolar seesaw permits a reconstruction of the Antarctic response to the northern millennial and sub-millennial scale variability over MIS 5. However, we show that when ice sheets are extensive, Antarctica does not necessarily warm during the whole GS as the thermal bipolar seesaw model would predict.

1 Introduction

Continental, marine and polar paleoclimate records preserve abundant evidence that a series of abrupt climate events at millennial scale occurred during the last glacial

CPD

6, 135–183, 2010

Millennial and sub-millennial scale climatic variations

E. Capron et al.

Title Page

Abstract

Introduction

Conclusions

References

Tables

Figures



Back

Close

Full Screen / Esc

Printer-friendly Version

Interactive Discussion



**Millennial and
sub-millennial scale
climatic variations**

E. Capron et al.

Title Page

Abstract

Introduction

Conclusions

References

Tables

Figures



Back

Close

Full Screen / Esc

Printer-friendly Version

Interactive Discussion



period (~18–110 kyr before present, hereafter ka) with a global expression (Voelker, 2002). These so-called “Dansgaard-Oeschger” (DO) events were first described and numbered in the deep Greenlandic ice cores from Summit back to 100 ka (72° 34′ N, 37° 37′ W, GISP2 and GRIP; Dansgaard et al., 1993; Grootes et al., 1993; GRIP-members, 1993). GISP2 and GRIP $\delta^{18}\text{O}_{\text{ice}}$ records highlight millennial scale variability related to the succession of warm interstadials (hereafter noted GIS for Greenland InterStadial) and cold stadials (GS for Greenland Stadial; Dansgaard et al., 1993).

The “iconic” DO event structure is depicted as a GIS, beginning with an abrupt warming of 8 to 16 °C mean annual surface temperature amplitude within few decades (Severinghaus et al., 1998; Lang et al., 1999; Landais et al., 2004a; Huber et al., 2006; Landais et al., 2006; see also Wolff et al., 2009a for a review). The GIS is then usually characterized by a gradual cooling phase lasting several centuries and its end is marked by a rapid cooling towards a relatively stable cold phase (GS) that persists over several centuries to a thousand of years. This description originates mainly from DO events occurring over Marine Isotopic Stage 3 (MIS 3, 30–60 ka; see Voelker (2002) for a review) that benefits from a robust chronology (Fig. 1; e.g., Wang et al., 2001; Shackleton et al., 2003; Fairbanks et al., 2005; Svensson et al., 2008).

The DO event signature is recorded in both continental and marine archives from high northern latitudes to the tropics (e.g., Bond et al., 1992; Chapman and Shackleton, 1999; Sanchez-Goñi et al., 2000; Sanchez-Goñi et al., 2002; Genty et al., 2003; Wang et al., 2008). This global characteristic is also illustrated by abrupt changes in atmospheric methane (CH_4) concentrations inferred from air trapped in ice associated with Greenland temperature shifts (e.g., Chappellaz et al., 1993; Flückiger et al., 2004; Huber et al., 2006; Loulergue et al., 2008).

A dynamical combination between ocean, cryosphere (continental ice sheets and sea ice cover), vegetation and atmosphere is at play during this millennial scale variability (Hendy and Kennett, 1999; Peterson et al., 2000; Kiefer et al., 2001; Wang et al., 2001; Broecker, 2003; Steffensen et al., 2008) but the triggering processes of such a variability are still under discussion (Wunsch, 2006; Friedrich et al., 2009). Cur-

rent theories point to external forcing mechanisms such as periodic changes in solar activity (Bond et al., 1992; Braun et al., 2008), periodic calving of ice sheets (van Kreveld et al., 2000) and to internal oscillations of the ice sheet-ocean-atmosphere system through freshwater perturbations (Broecker, 1990; MacAyeal, 1993; Ganopolski and Rahmstorf, 2001; Schulz et al., 2002a).

In Antarctic ice cores, millennial scale temperature changes are gradual and out of phase with their abrupt northern counterpart (Fig. 1; Bender et al., 1994; Blunier et al., 1998; Blunier and Brook, 2001; EPICA-community-members, 2006; Capron et al., 2010). Such a “bipolar seesaw” pattern is understood as reflecting changes in the strength of the Atlantic Meridional Oceanic Circulation (AMOC; Broecker, 1998). The physical mechanism for this bipolar seesaw pattern has been explored through a large panel of conceptual and numerical models of various complexities (e.g., Stocker et al., 1992; Rind et al., 2001; Vellinga and Wood, 2002; Knutti et al., 2004; Kageyama et al., 2009; Liu et al., 2009; Swingedouw et al., 2009). Using the simplest possible model, Stocker and Johnsen (2003) successfully described the Antarctic millennial variability in response to the abrupt temperature changes in the north by involving a southern heat reservoir associated with AMOC variations. Such an important role of the Southern Ocean for the bipolar seesaw mechanism is supported by marine records (Barker et al., 2009).

Our knowledge of millennial scale climatic evolution before MIS 3 is limited by lower resolution, as well as higher stratigraphic and dating uncertainties. Nevertheless, millennial scale variability is observed from the very beginning of the last glacial period (Cortijo et al., 1994; McManus et al., 1999; Eynaud et al., 2000; Oppo et al., 2001; Genty et al., 2003; Heusser and Oppo, 2003; NorthGRIP-community-members, 2004; Sprovieri et al., 2006; Meyer et al., 2008; Wang et al., 2008) and during previous glacial periods (McManus et al., 1999; Jouzel et al., 2007; Siddall et al., 2007; Loulergue et al., 2008).

The last glacial inception, known as MIS 5 (~73.5–130 ka; Shackleton, 1987) is a time period of great interest since it represents an intermediary stage between full

Millennial and sub-millennial scale climatic variations

E. Capron et al.

Title Page

Abstract

Introduction

Conclusions

References

Tables

Figures

◀

▶

◀

▶

Back

Close

Full Screen / Esc

Printer-friendly Version

Interactive Discussion



interglacial conditions and glacial conditions encountered during MIS 2–3. At that time, continental ice sheets are extending, corresponding to sea level variations from 20 to 60 m below present-day sea level (Waelbroeck et al., 2002) compared to –120 m during MIS 2–3. MIS 5 is also marked by a different orbital configuration with stronger eccentricity and therefore larger seasonal insolation changes compared to MIS 3 (Fig. 1).

The NorthGRIP ice core (Greenland, 75° 10' N, 42° 32' W; 2917 m above sea level (m.a.s.l.); present accumulation rate of 17.5 cm water equivalent per year (cm w.e. yr⁻¹)) expands the Summit records back to the last interglacial period (~123 ka) and offers high resolution (1 cm yr⁻¹) due to the basal melt limiting thinning processes (NorthGRIP c.-m., 2004) The $\delta^{18}\text{O}_{\text{ice}}$ profile unveiled GIS 23, 24, and 25 in the early time of the glacial period (~101–113 ka; Fig. 1; NorthGRIP c.-m., 2004). The discovery of only six abrupt climatic events during MIS 5 (GIS 20 to 25) reveals a longer pacing than the ~1.5 thousand of years (hereafter kyr) approximate DO event frequency suggested by Grootes and Stuiver (1997) for the later glacial and strongly debated since (e.g., Grootes and Stuiver, 1997; Schulz, 2002b; Rahmstorf, 2003; Ditlevsen et al., 2005; Ditlevsen et al., 2007).

The ice core drilled within the European Project for Ice Coring in Antarctica (EPICA) in the interior of Dronning Maud Land (hereafter, denoted EDML, 75° S, 0° E, 2892 m a.s.l., present accumulation rate of 6.4 cm w.e. yr⁻¹) which faces the South Atlantic Ocean provides a resolution of ~30 yr during MIS 3 and of ~60 yr during MIS 5. This makes the EDML core particularly suitable for studying millennial scale climatic variations in Antarctica. During MIS 3, it was shown that the amplitudes of EDML Antarctic Isotopic Maxima (AIM) are linearly related to the duration of the concurrent GS (EPICA-community-members, 2006). Moreover, taking advantage of a new common timescale between EDML and NorthGRIP ice cores based on the global signals of atmospheric composition changes, Capron et al. (2010) depict a bipolar seesaw structure during MIS 5 including the first GIS 25 (Fig. 2). They reveal that during the long GS 22 the corresponding AIM 21 amplitude does not reach the warming expected from the linear relationship observed during MIS 3.

Millennial and sub-millennial scale climatic variations

E. Capron et al.

Title Page

Abstract

Introduction

Conclusions

References

Tables

Figures

◀

▶

◀

▶

Back

Close

Full Screen / Esc

Printer-friendly Version

Interactive Discussion



**Millennial and
sub-millennial scale
climatic variations**

E. Capron et al.

[Title Page](#)[Abstract](#)[Introduction](#)[Conclusions](#)[References](#)[Tables](#)[Figures](#)[⏪](#)[⏩](#)[◀](#)[▶](#)[Back](#)[Close](#)[Full Screen / Esc](#)[Printer-friendly Version](#)[Interactive Discussion](#)

Hereafter, we combine the full climatic information available from the NorthGRIP and EPICA ice cores in order to provide a complete description of the abrupt climatic oscillations recorded in the polar regions over MIS 5 in comparison to MIS 3. In Sect. 2, we present the common timescales used for the NorthGRIP and EPICA ice cores over MIS 3 and MIS 5. Section 3 deals with new high resolution measurements of EDML $\delta^{18}\text{O}_{\text{ice}}$ and of NorthGRIP $\delta^{15}\text{N}$ and $\delta^{40}\text{Ar}$ which are then used to characterize MIS 5 GS and GIS in terms of structure, temperature amplitude and their relationships with their Antarctic counterparts. In particular, we bring new evidence of sub-millennial scale variability at the onset and the end of the MIS 5 long interstadials. We then discuss the robust features and peculiarities of GIS events of MIS 3 and MIS 5 in relationship with their different climate background (i.e. CO_2 concentration, ice volume, orbital contexts) in Sect. 4. Finally, in Sect. 5, we test the general applicability of the thermal bipolar seesaw concept for the entire glacial period by comparing our results with north-south time-series generated through the conceptual model of Stocker and Johnsen (2003).

2 Timescale synchronisation and past temperature reconstruction of North-GRIP and EDML ice cores

2.1 Synchronising NorthGRIP and EDML ice cores

An accurate timescale is necessary to characterize the duration and pacing of climatic events and the sequence of events between the northern and the Southern Hemispheres.

For MIS 3, we use the most recent GICC05 age scale (Greenland Ice Core Chronology 05) extended back to 60 ka (Svensson et al., 2008) for the NorthGRIP ice core. GICC05 is a time scale based on annual layer counting and has been successfully compared with absolutely dated reference horizons in the 0–60 ka period (Svensson et al., 2008; Fleitmann et al., 2009). A synchronization performed using the isotopic

composition of atmospheric oxygen ($\delta^{18}\text{O}_{\text{atm}}$) and CH_4 records from air entrapped in EDML and NorthGRIP ice (e.g., Bender et al., 1994; Blunier et al., 1998) enables Blunier et al. (2007) to place the two ice cores on the same timescale. From 25 to 50 ka, the maximum uncertainty between the two records is estimated to reach 500 yr at the onset of GIS 12.

To study MIS 5, we transferred the NorthGRIP record onto the EDML1 timescale between 80 and 123 ka using also a $\delta^{18}\text{O}_{\text{atm}}$ and CH_4 gas synchronisation (Capron et al., 2010). EDML1 is derived from the EDC3 official chronology (Parrenin et al., 2007a; Ruth et al., 2007; Severi et al., 2007). The new EDML-NorthGRIP timescale enables us to quantify the exact phasing between the onsets of AIM and GIS with an accuracy of a few centuries except for the onset of GIS 25, where the uncertainty is higher than 1 kyr. Unlike for MIS 3, we are not using an absolute timescale for MIS 5 as focussing on the duration and sequence of events only requires a relative timescale. NorthGRIP basal melting induces a timescale almost linearly proportional to depth by reducing the ice thinning (NorthGRIP c.-m., 2004; Dahl-Jensen et al., 2003). For the new EDML-NorthGRIP age-scale, we obtain a smooth evolution of age as a function of depth with less than 10% deviation from the slope deduced from the age/depth relationship of the NorthGRIP glaciological timescale (NorthGRIP c.-m., 2004). We thus consider our age markers as being consistent with ice flow conditions at the NorthGRIP site.

This timescale can be compared to independent chronologies from other paleoclimatic archives. In the North Atlantic region, marine cores show rapid cooling events (C events) (McManus et al., 1994) that were associated with the GS (i.e. event C 24 is associated with GS 25, McManus et al., 1994; NorthGRIP c.-m., 2004; Rousseau et al., 2006). Using such association, NorthGRIP DO event duration is compared to the one deduced from two marine sediment cores: i) MD95-2042, providing an age scale with two absolute age markers derived from the Hulu cave between 115 and 81 kyr (Shackleton et al., 2003) and ii) NEAP18K, whose age model was constructed by correlation of the benthic $\delta^{18}\text{O}$ records with an orbitally tuned $\delta^{18}\text{O}$ stratigraphy (Shackleton and

Millennial and sub-millennial scale climatic variations

E. Capron et al.

Title Page

Abstract

Introduction

Conclusions

References

Tables

Figures

⏪

⏩

◀

▶

Back

Close

Full Screen / Esc

Printer-friendly Version

Interactive Discussion



Pisias, 1985).

Then, the same exercise is carried out by comparing our age-scale with the chronology from a lacustrine sediment core from Lago grande di Monticchio (Brauer et al., 2007) whose chronology is based on lamination counting. Finally, assuming synchronous climatic shifts at low and high latitudes enables us to compare rapid event succession recorded in ice cores through independent dating from speleothem records (i.e., Wang et al., 2001, 2008). Such a comparison is difficult because few speleothem records display a clear sequence of rapid events over MIS 5 except the record from Sanbao cave on which we can identify the onset of each GIS event (Wang et al., 2008).

Uncertainties on DO event durations (i.e. duration of GIS plus GS) obtained from the comparison of the five records are summarized in Table 1. In the following we limit our study to DO events 24, 23, 22 and 21 since the EDML-NorthGRIP synchronisation lacks of robust chronological constraints around DO event 25 (Capron et al., 2010). The uncertainties associated with the durations of DO events 24, 23, 22 and 21, represent less than 13 % of the duration of each DO event. This general agreement makes the possibility of a large (greater than 1.3 kyr) error in interstadial duration unlikely and provides firm bases to confidently analyse the interstadial structure and pacing of these events over MIS 5.

2.2 Past temperature reconstructions

The stable isotopic composition of precipitation at mid and high latitudes is related to local air temperature through the so-called spatial slope (Dansgaard, 1964) with an average of $0.67\text{‰}-\delta^{18}\text{O}$ per $^{\circ}\text{C}$ slope in Greenland (Johnsen et al., 1989) and $0.75\text{‰}-\delta^{18}\text{O}$ per $^{\circ}\text{C}$ slope in Antarctica (Lorius and Merlivat, 1977, Masson-Delmotte et al., 2008). This spatial slope, which results from air mass distillation processes, can be used as a surrogate for the temporal slope and may vary over time due to past changes in evaporation conditions or atmospheric transport. However, the ice isotopic composition as a tool for past temperature reconstructions (Dansgaard, 1964) has to be taken with a careful look. Indeed, the hypothesis of similar spatial and temporal slopes is

Millennial and sub-millennial scale climatic variations

E. Capron et al.

Title Page

Abstract

Introduction

Conclusions

References

Tables

Figures



Back

Close

Full Screen / Esc

Printer-friendly Version

Interactive Discussion



only valid if certain assumptions are satisfied, in particular those concerning the origin and seasonality of the precipitation (Jouzel et al., 1997).

In fact, past Greenland temperature reconstructions based on the spatial isotope-temperature slope have been challenged by alternative paleothermometry methods such as i) the inversion of the borehole temperature profile (e.g., Dahl-Jensen et al., 1998; Cuffey and Clow, 1995; Johnsen et al., 1995) and ii) the thermal diffusion of air in the firn arising during abrupt climate changes (Severinghaus et al., 1998). The quantitative interpretation of $\delta^{18}\text{O}_{\text{ice}}$ in term of temperature variations using this spatial relationship leads to a systematic underestimation of temperature changes (Jouzel, 1999). The amplitudes and shapes of temperature changes can be biased by past changes in precipitation seasonality (Fawcett et al., 1996; Krinner et al., 1997), changes in moisture sources during rapid events (Charles et al., 1994; Boyle, 1997; Masson-Delmotte et al., 2005) and surface elevation (i.e. Vinther et al., 2009).

By contrast, available information suggest that reconstruction of local surface temperature in Antarctic ice cores using the present-day spatial relationship between isotopic composition of the snow and surface temperature (“isotopic thermometer”) is correct, with a maximum associated uncertainty of 20% at the glacial-interglacial scale (Jouzel et al., 2003). As a consequence, the isotopic thermometer is commonly used to quantify past changes in temperature based on the stable isotopic composition measured in deep Antarctic ice cores (e.g., EPICA c.-m., 2006; Jouzel et al., 2007). More recently, a modelling study dedicated to the stability of the temporal isotope-temperature slope suggests that the classical interpretation of the ice core stable isotopes on EDC may lead to an underestimation of past temperatures for periods warmer than present conditions (Sime et al., 2009).

2.2.1 Greenland temperature reconstruction

Measurements of the isotopic composition of nitrogen ($\delta^{15}\text{N}$) and/or argon ($\delta^{40}\text{Ar}$) from air trapped in ice cores provide independent quantitative reconstructions of abrupt local temperature changes (Severinghaus et al., 1998; Lang et al., 1999; Severinghaus and

Millennial and sub-millennial scale climatic variations

E. Capron et al.

Title Page

Abstract

Introduction

Conclusions

References

Tables

Figures

◀

▶

◀

▶

Back

Close

Full Screen / Esc

Printer-friendly Version

Interactive Discussion



**Millennial and
sub-millennial scale
climatic variations**

E. Capron et al.

Title Page

Abstract

Introduction

Conclusions

References

Tables

Figures



Back

Close

Full Screen / Esc

Printer-friendly Version

Interactive Discussion



Brook, 1999; Landais et al., 2004a; Landais et al., 2004b; Landais et al., 2004c; Huber et al., 2006). Trapped-air $\delta^{15}\text{N}$ variations are only produced by firn isotopic fractionation due to gravitational and thermal diffusion since atmospheric $\delta^{15}\text{N}$ is constant over the past million years (Mariotti, 1983). The combined use of $\delta^{15}\text{N}$ and $\delta^{40}\text{Ar}$ data together with the modelling of physical processes (densification, temperature and gas diffusion) enable the estimation of abrupt surface temperature magnitudes with an accuracy of 2.5°C (Landais et al., 2004a).

Table 2 and Fig. 2 display a synthesis of all available $\delta^{15}\text{N}$ -based temperature estimates for GIS amplitudes. Abrupt warmings of GIS 8 to GIS 17 vary between 8 to 15°C (Huber et al., 2006). Over MIS 5, GIS 23 and 24 amplitudes show a warming of 10°C and 16°C , respectively (Landais et al., 2006). Following the approach of Landais et al. (2004a), the GIS 21 onset is marked by a warming of 11°C quantified with $\delta^{15}\text{N}$ (Capron et al., 2010) and new $\delta^{40}\text{Ar}$ data (Fig. 3). New high resolution gas measurements over GIS 22 reveal a weak $\delta^{15}\text{N}$ variation (0.063‰) corresponding to a maximum warming amplitude of 5°C (Fig. 3).

Compared to the classical isotope–temperature relationship, the temporal-calculated slope between changes in $\delta^{18}\text{O}$ and in $\delta^{15}\text{N}$ -derived temperature at the onset of GIS events is systematically lower and varies from 0.31 to $0.59\text{‰}/^\circ\text{C}$. Previous studies have suggested an effect of obliquity, ice-sheet on the temporal $\delta^{18}\text{O}_{\text{ice}}/\text{temperature}$ slope mainly via the seasonality of the precipitation and/or moisture source (Denton et al., 2005; Masson-Delmotte et al., 2005; Flückiger et al., 2008). Here, we do not find any systematic relationship between the evolution of the temporal slope and long term evolution of ice sheets and orbital parameters. We suggest instead that the temporal slope and thus seasonality and/or moisture source change at the GIS scale.

It should be noted that NorthGRIP temperature change over DO events is perhaps not a reference for the whole Greenland climate: despite being only 325 km apart, NorthGRIP and GISP2 present different temperature changes associated with GIS 19 and 20. While the temperature changes are similar for GIS 20 onset (12°C), the onset of GIS 19 presents a temperature change of 16°C and 14°C at NorthGRIP and GISP2,

respectively. This partly reflects different shifts in the $\delta^{18}\text{O}_{\text{ice}}$ variation. These regional differences are linked to a “continentality” effect at the NorthGRIP location which does not exist at the GISP2 site. The NorthGRIP $\delta^{18}\text{O}_{\text{ice}}$ profile should therefore be used to qualitatively discuss the relative amplitudes and shapes (Johnsen et al., 2001; North-GRIP c.-m., 2004).

2.2.2 Antarctica temperature reconstruction

Only one study in Antarctica so far has used the gas fractionation paleothermometry method and showed a temperature change consistent within 20% of the classical interpretation of water stable isotope fluctuations (Caillon et al., 2001). Indeed, the smoother shape of millennial scale temperature changes prevents the use of the isotopic composition of the air to infer local temperature change during AIM events. The $\delta^{18}\text{O}_{\text{ice}}$ based temperature reconstruction may however be improved by using the deuterium excess data ($d\text{-excess} = \delta D - 8 \times \delta^{18}\text{O}_{\text{ice}}$; Dansgaard, 1964) which allows to correct for the changes in moisture source conditions (e.g., Stenni et al., 2001; Vimeux et al., 2002; Stenni et al., 2010).

Here we use two different temperature reconstructions to characterize AIM warming amplitudes in East Antarctica. First, new high resolution and already published EDML $\delta^{18}\text{O}_{\text{ice}}$ and EDC δD profiles (Fig. 3) are corrected for global seawater isotopic composition (Bintanja et al., 2005) following Jouzel et al. (2003) and then converted to past temperatures using the observed spatial slope of $0.82 \times \delta^{18}\text{O}_{\text{ice}}$ per $^{\circ}\text{C}$ for EDML (Oerter et al., 2004) and $6.04 \times \delta D$ per $^{\circ}\text{C}$ for EDC (Lorius and Merlivat, 1977; Masson Delmotte et al., 2008). These temperatures are corrected from elevation variations and changes in ice origin (upstream and elevation correction; for EDML: Huybrechts et al., 2007; for EDC: Parrenin et al., 2007b). It results in a $\sim 0.2^{\circ}\text{C}$ difference between the temperature reconstruction with only correction for the global seawater isotopic composition and the one taking into account the upstream correction in addition.

Secondly, we use the EDML and EDC temperature profiles derived using d-excess

Millennial and sub-millennial scale climatic variations

E. Capron et al.

Title Page

Abstract

Introduction

Conclusions

References

Tables

Figures

◀

▶

◀

▶

Back

Close

Full Screen / Esc

Printer-friendly Version

Interactive Discussion



**Millennial and
sub-millennial scale
climatic variations**E. Capron et al.

[Title Page](#)[Abstract](#)[Introduction](#)[Conclusions](#)[References](#)[Tables](#)[Figures](#)[⏪](#)[⏩](#)[◀](#)[▶](#)[Back](#)[Close](#)[Full Screen / Esc](#)[Printer-friendly Version](#)[Interactive Discussion](#)

data recently published by Stenni et al. (2010). Based on isotopic profiles corrected from sea water isotopic composition and upstream effects, they estimate changes in source conditions and site temperature at both sites (Stenni et al., 2001; Masson-Delmotte et al., 2004). These site temperature reconstructions are expected to be more robust because they account for changes in evaporation conditions. However, for some rapid events, this “inverted” temperature is noisier and makes the beginning and the end of the warming more difficult to identify (Fig. 3; Stenni et al., 2010). Thus, both “classical” and “site” temperature reconstructions are used for EDC and EDML to identify AIM and associated warming amplitudes.

The AIM temperature change amplitudes are presented in Table 2. We estimate a maximum uncertainty of 0.4 °C based on i) the warming amplitude difference between the two reconstructions and ii) the determination of the minima and maxima for Antarctic temperature changes. The moisture correction does not have any major impact on AIM amplitudes nor on their shapes.

Note that Antarctic events with amplitudes of less than 1‰ (equivalent to 0.5 °C) remain delicate to interpret since the δ -excess corrections add noise to the temperature reconstruction. We choose hereafter to discuss only small events that have a Greenland counterpart and to ignore the other small $\delta^{18}\text{O}_{\text{ice}}$ fluctuations.

3 Structure of MIS 5 abrupt climate variability

The exceptionally long duration of the GIS during MIS 5 reveals an additional variability within the classical GIS/GS succession. Three types of sub-millennial scale events are identified: i) abrupt cooling phases during GIS 24, ii) short-lived and sharp warming preceding GIS 21 and GIS 23 and iii) abrupt warming during the cooling phase of GIS 21.

3.1 The singular case of GIS 24

GIS 24 presents a “squared” structure beginning with an abrupt temperature warming of 16 °C (Landais et al., 2006) and ending 3.2 kyr later by a sudden return to stadial conditions (Fig. 4). The warm phase is punctuated by rapid cold events since the slow $\delta^{18}\text{O}_{\text{ice}}$ decrease is interrupted by a first drop of $\delta^{18}\text{O}_{\text{ice}}$ by 3‰ lasting 200 yr before a return to interstadial $\delta^{18}\text{O}_{\text{ice}}$ level. A second cooling phase occurs 500 yr later with a 2.5‰- $\delta^{18}\text{O}_{\text{ice}}$ decrease. Finally, a stable phase is observed during 500 yr followed by the final return to stadial conditions in less than 200 yr. The abrupt changes in $\delta^{18}\text{O}_{\text{ice}}$ are due to changes in surface temperature as confirmed by the associated two 0.04‰ drops in $\delta^{15}\text{N}$ coincident with $\delta^{18}\text{O}_{\text{ice}}$ abrupt variations (Fig. 4).

The first rapid cooling over GIS 24 includes most probably lower latitudes counterparts as documented by a simultaneous drop in CH_4 concentration during 150–200 yr. In addition, sub-millennial scale variations in $\delta^{18}\text{O}$ of O_2 have been identified during GIS 24 (Capron et al., 2010) reflecting significant changes of biosphere and hydrological cycles at these short timescales (Landais et al., 2010).

Finally, GIS 24 is marked by a unique sub-millennial structure during the last glacial period: no other GIS is interrupted by such short cold events. We can only compare it with the 8.2 ka-event that occurred at the beginning of the Holocene (Alley et al., 1997; Leuenberger et al., 1999; Kobashi et al., 2007; Thomas et al., 2007). These cold events occur during two different periods of transition (glacial inception for the cold events of GIS 24, end of deglaciation for the 8.2 ka-event), but both at a time when ice sheets are relatively small. The AMOC during transitional periods is expected to present rapid instabilities leading to sub-millennial variability because of strong modifications of the freshwater input linked to i) freshwater discharge (von Grafenstein et al., 1998; Clarke et al., 2004) and/or ii) enhanced precipitation (Khodri et al., 2001) and favoured by small ice sheets (Eisenman et al., 2009).

Title Page

Abstract

Introduction

Conclusions

References

Tables

Figures



Back

Close

Full Screen / Esc

Printer-friendly Version

Interactive Discussion



3.2 Precursor-type peak events

The NorthGRIP isotopic profile contains dramatic reversals in $\delta^{18}\text{O}_{\text{ice}}$ before the two longest GIS of the entire glacial period: GIS 21 and GIS 23 (Fig. 5). The first occurs within 200 yr with a 2.2‰ variation in $\delta^{18}\text{O}_{\text{ice}}$. After a short (100 yr) return to cold conditions, GIS 21 onset occurs with a 4.2‰ increase in $\delta^{18}\text{O}_{\text{ice}}$. Such a precursor-type structure is also visible before GIS 23 onset: the $\delta^{18}\text{O}_{\text{ice}}$ rises by 3.8‰ in 125 yr at ~ 102.5 ka and then drops by 3.6‰ in 100 yr (hereafter, denoted as GIS 23b). The return to stadial conditions lasts ~ 300 yr before $\delta^{18}\text{O}_{\text{ice}}$ increases by 3‰ at the onset of GIS 23.

The occurrence of precursor events is confirmed by parallel $\delta^{18}\text{O}_{\text{ice}}$ variations measured in GRIP and GISP2 cores (Johnsen et al., 1992; Grootes and Stuiver, 1997; Gratchev et al., 2007) and by their detection in high-resolution records of $\delta^{15}\text{N}$ data and CH_4 . The precursor-type peak event leading GIS 23 exhibits a 200 ppbv variation in CH_4 and a 0.050‰ rapid increase in $\delta^{15}\text{N}$. The reversal prior to GIS 21 is weaker in the NorthGRIP $\delta^{18}\text{O}_{\text{ice}}$ profile (2.2‰) than GISP2 (3.4‰) whereas NorthGRIP $\delta^{15}\text{N}$ data over this reversal indicate a 0.08‰ variation in NorthGRIP comparable to the $\delta^{15}\text{N}$ variation of 0.09‰ measured in GISP2 (Gratchev et al., 2007).

Note that these very short $\delta^{18}\text{O}_{\text{ice}}$ variations are not only visible during MIS 5. Indeed, the sequence of DO events 13 to 17 during MIS 3 is also extremely unstable with short temperature peaks of 200–400 yr accompanied by fast shifts in CH_4 concentration (Blunier and Brook, 2001; Flückiger et al., 2004; Huber et al., 2006). This highlights that abrupt climatic variability over the glacial period is more complex than the millennial scale variations expressed by a GIS/GS succession.

3.3 Rebound-type events

At the end of the regular cooling phase of GIS 21, $\delta^{18}\text{O}_{\text{ice}}$ increases abruptly ($\sim 2\%$ in less than 100 yr) 1.2 kyr before the sharp return to stadial conditions (Fig. 6). The

[Title Page](#)[Abstract](#)[Introduction](#)[Conclusions](#)[References](#)[Tables](#)[Figures](#)[◀](#)[▶](#)[◀](#)[▶](#)[Back](#)[Close](#)[Full Screen / Esc](#)[Printer-friendly Version](#)[Interactive Discussion](#)

**Millennial and
sub-millennial scale
climatic variations**

E. Capron et al.

large scale imprint of the GIS 21 sub-event is detected through GISP2 high resolution CH_4 data (showing a 71 ppbv increase in 140 yr; Grachev et al., 2009). This “rebound” pattern is identical in $\delta^{18}\text{O}_{\text{ice}}$ magnitude, duration and structure to GIS 22. GIS 23 ends with a smooth cooling making impossible to clearly identify a GS 23 phase. Finally, the GIS 23-22 sequence of events shows exactly the same type of structure as the one observed over GIS 21.

Rebound-type events are not only restricted to MIS 5 as they are also occurring at the end of GIS 11, 12 and 16 (Fig. 6). GIS 13 also appears as a rebound event after the long GIS 14 without a clear GS 14. These rebound-type features are therefore recurrent over the glacial period and except for GIS 11 and GIS 12, are associated with the precursor-type events before GIS.

We also observe that rebound-type events are occurring at the end of a particularly long cooling phase during the GIS. Figure 6 highlights a linear link between the duration of GIS gradual cooling and the rebound event duration from multi-millennial (e.g. sequence of GIS 22–23 events and GIS 21) to few century timescales (e.g. GIS 11 and 16).

3.4 Antarctic sub-millennial scale variability

The new detailed $\delta^{18}\text{O}_{\text{ice}}$ measurements on the EDML ice core allow the identification of an Antarctic counterpart to the stadial phase between the precursor and GIS 23, as a 1‰ $\delta^{18}\text{O}_{\text{ice}}$ variation within a few decades (Fig. 3). This AIM shows a $\sim 1^\circ\text{C}$ temperature increase simultaneous to the cold Greenland phase lasting ~ 400 yr. As for the rapid variability during GIS 24, Antarctic $\delta^{18}\text{O}_{\text{ice}}$ and T_{site} reconstructions also exhibit sub-millennial counterparts. After reaching a relative temperature maximum corresponding to AIM 24, the general trend shows a regular decrease interrupted by a 1 kyr plateau that may correspond with the short cold spell occurring during GIS 24 (Figs. 3 and 4).

Note that we do not identify an Antarctic counterpart to the cold phase between the precursor and GIS 21 (Fig. 3). Two hypotheses could explain such a result: i) a lack

[Title Page](#)[Abstract](#)[Introduction](#)[Conclusions](#)[References](#)[Tables](#)[Figures](#)[Back](#)[Close](#)[Full Screen / Esc](#)[Printer-friendly Version](#)[Interactive Discussion](#)

of resolution in the EDML $\delta^{18}\text{O}_{\text{ice}}$ profile (ii) the damping of Greenland temperature signals when transferred to Antarctica through the Southern Ocean.

4 Discussion

4.1 Millennial to sub-millennial GIS variability

5 The detailed analysis of the long GIS of MIS 5 reveals sub-millennial scale variations during the warm phase of rapid events. During GIS 21 and GIS 23, we depict a specific structure composed of a precursor-type warming event leading the GIS and a “rebound-type” abrupt event before the GIS abruptly ends. Such a structure is re-
10 current during MIS 3 at shorter timescales and Fig. 6 displays a linear relationship between the durations of the “rebound-type event” and of the preceding GIS regular cooling.

Here, we present the mechanisms for triggering this sub-millennial variability. Different factors are currently proposed for explaining the DO climatic variability: i) millennial scale CO_2 levels influencing the amplitude of rapid events (Liu et al., 2009), ii) ice sheet
15 size controlling iceberg discharges (MacAyeal, 1993) and the North Atlantic hydrological cycle (Eisenman et al. 2009), iii) 65°N insolation affecting temperature, seasonality, hydrological cycle and ice sheet growth in the high latitudes (e.g., Gallée et al., 1992; Crucifix and Loutre, 2002; Khodri et al., 2003; Flückiger et al., 2004). These influences may also be enhanced through feedbacks. In particular, sea ice extent variations are
20 often given as trigger for abrupt warming oscillations (Wang and Mysak, 2006) or in explaining their amplitude (Li et al., 2005).

The Byrd ice core provides evidence for millennial scale CO_2 variations of about 16 ppm that precede the largest and longest abrupt events back to 80 ka (Ahn and Brook, 2008). While these CO_2 variations may be related to the length of the GIS,
25 a study of the CO_2 influence on the sub-millennial scale variability over MIS 5 would necessitate high resolution CO_2 data further back in time.

Millennial and sub-millennial scale climatic variations

E. Capron et al.

Title Page

Abstract

Introduction

Conclusions

References

Tables

Figures



Back

Close

Full Screen / Esc

Printer-friendly Version

Interactive Discussion



**Millennial and
sub-millennial scale
climatic variations**E. Capron et al.

[Title Page](#)[Abstract](#)[Introduction](#)[Conclusions](#)[References](#)[Tables](#)[Figures](#)[Back](#)[Close](#)[Full Screen / Esc](#)[Printer-friendly Version](#)[Interactive Discussion](#)

A more probable explanation for the occurrence of the sub-millennial variability is the link with ice sheet volume. The length of the GIS displayed on Fig. 6 can easily be related to the mean sea level with the long GIS 23 and 21 being associated with the highest sea level while GIS 11, 12, 14 and 16 are associated with lower sea level during MIS 3 (Fig. 1). Such a link between the GIS length and sea level is expected from a simple Binge-Purge mechanism (MacAyeal, 1993): largest ice-sheets are expected to be easier to destabilize. However, such a Binge-Purge mechanism is unlikely to explain the existence of precursor-type events. Indeed, the strong sub-millennial scale variability observed during GIS 21, 23, 24 and 16 occurs during relative ice sheet volume minima. A more plausible mechanism for these precursor events would be that small ice sheets are more sensitive than large ice sheets to a modification in the local radiative budget i.e. in response to a strong 65° N summer insolation ice sheet melting could lead to fast changes in the AMOC intensity by releasing freshwater intermittently.

The influence of the Milankovitch insolation forcing on the sub-millennial variability should also be discussed (Fig. 6). During MIS 5, GIS 21 precursor-type event is in phase with the relative maxima in summertime insolation at 65° N and the GIS 23 precursor-type event corresponds to a delay of ~2.5 kyr with the preceding insolation maxima. During MIS 3, we again observe that precursor-type events GIS 14 and 16 are associated with secondary insolation maxima. On the contrary, GIS 11 and 12 are not preceded by a precursor and occur at a time without a marked anomaly in 65° N summer insolation. This strongly suggests a link between insolation maximum and the presence of a precursor before a GIS.

Very short (less than 50 yr) precursor-type temperature events in Greenland have been generated in simulations obtained from a fully coupled ocean-atmosphere general circulation climate model in response to an abrupt cessation of freshwater forcing (Otto-Bliesner and Brady, 2010). These results suggest that the state of the AMOC from an “off” to “on” mode may be very unstable. Our data imply that such instabilities may be favoured during strong 65° N summertime insolation. Indeed, stronger radiative forcing enhances ice melting and the North Atlantic water cycle and consequently, modifies

the North Atlantic freshwater flow and the AMOC intensity.

Again, the influence of insolation can be used for the occurrence of rebound-type events at the end of GIS 23, 21, 16 and 14. The regular and long cooling phases of these GIS take place in a context of a decreasing 65° N summertime insolation and an active AMOC. The rebound at the end of the GIS should be explained by an enhancement of the AMOC through perturbation in the salinity budget. Indeed, the decreasing northern insolation should lead to an increase in sea ice formation and a reduction in precipitation amount/runoff that should increase salinity in the North Atlantic region.

4.2 The bipolar seesaw pattern

In the above discussion, we described rapid climatic variations over Greenland. Here, we use our common dating of Antarctic and Greenland ice cores to study the north-south millennial scale variability over the whole glacial period and test the general applicability of the conceptual thermal bipolar seesaw of Stocker and Johnsen (2003) especially over the new types of rapid events identified over MIS 5.

4.2.1 Millennial scale variations

Synchronised EDML and NorthGRIP isotopic records emphasized the close link between the amplitude of MIS 3 AIM warming and their concurrent stadial duration in Greenland (EPICA c.-m., 2006). To complete this description we have added on Fig. 7 DO/AIM 2, 21, 23 and 24 using our MIS 5 timescale (EPICA c.-m., 2006; Capron et al., 2010). Finally, DO/AIM events 18, 19 and 20 have also been added despite a lack of a precise north-south common age scale over this period (Fig. 7).

EPICA c.-m. (2006) reveal a linear dependency between the amplitude of the AIM warming and the duration of the concurrent stadial in the North. We observe that the linear fit established over MIS 3 also captures the characteristics of DO/AIM events 19, 20, 23 and 24 (Capron et al., 2010) but does not apply for DO/AIM events 2, 18 and 21.

Title Page

Abstract

Introduction

Conclusions

References

Tables

Figures

◀

▶

◀

▶

Back

Close

Full Screen / Esc

Printer-friendly Version

Interactive Discussion



Millennial and sub-millennial scale climatic variations

E. Capron et al.

In fact, these DO exceptions are all preceded by exceptionally long cold periods in the NorthGRIP record. Exceptionally high temperature amplitudes would be expected from the linear regression as a GS duration of 4 kyr would correspond to an AIM warming of $\sim 5^\circ\text{C}$, much stronger than the observed warming amplitude if the AIM 2, 18 and 21.

A linear relationship with a constant slope fails to reproduce the AIM amplitude vs. GS duration for the long GS which supports the thermal bipolar seesaw concept. Indeed, Stocker and Johnsen (2003) predict that for long period of reduced AMOC (equivalent to GS duration in their model) a new equilibrium is reached and the Antarctic warming would eventually end. This type of situation could be relevant for the long DO/AIM 21, while the other DO/AIM events may be too short for an equilibrium to be reached.

Hereafter, we make sensitivity test using the equation developed in Stocker and Johnsen (2003):

$$\Delta T_S(t) = -(1/\tau) \int [T_N(t-t')e^{-t'/\tau}] dt' \quad (1)$$

Where $\Delta T_S(t)$ represents the time-dependant temperature variation in the Southern Hemisphere, τ is the characteristic timescale of the heat reservoir in the Southern Hemisphere, T_N denotes the time-dependent temperature anomaly of the northern end of the bipolar seesaw. This equation predicts the southern temperature in response to climate signals in the North Atlantic region. The integral form associated with a characteristic time τ for the southern heat reservoir permits to describe the dampened temperature changes in the Southern Ocean in response to abrupt temperature changes in the North Atlantic. Following Stocker and Johnsen (2003), a value of -1 for T_N stands for a GS associated with an “off” mode of the AMOC. To model the abrupt GS/GIS transition associated with resumption of the AMOC, T_N changes from -1 to $+1$. A characteristic timescale τ of about 1000–1500 yr has been determined to fit the Byrd temperature curve using the GRIP data as input.

On Fig. 7, we display ΔT_S simulations obtained with i) changes in T_N of $-1/+1$ and $-2/+2$ and ii) τ varying between 500 and 1500 yr. The different results clearly illustrate

Title Page

Abstract

Introduction

Conclusions

References

Tables

Figures

◀

▶

◀

▶

Back

Close

Full Screen / Esc

Printer-friendly Version

Interactive Discussion



**Millennial and
sub-millennial scale
climatic variations**

E. Capron et al.

a saturation level reached in the south when Greenland stadials are particularly long (more than 2000 yr). The simulations with the largest T_N amplitude ($-2/+2$) permit to fit the AIM amplitude/NorthGRIP duration for MIS 5 events, DO 8, 12 and 19. However, it is impossible to simulate the behaviours of all events of the glacial period with a fixed amplitude for T_N even with very large modifications of τ .

Our analysis suggests that larger amplitudes for T_N are needed to explain the Antarctic behaviour when ice sheets are smaller. However, such interpretation is based on the hypothesis that the Antarctic temperature reflects the change in the Southern Ocean. This may not be systematically true since a recent study based on a marine sediment core from the Southern Ocean evidences similar Sea Surface Temperature (SST) increases during C 20 and C 24 whereas AIM 21 amplitude is clearly larger than AIM 23 one in EPICA ice cores (Govin et al., 2009). As a consequence, this change in Antarctic behaviour in regard to rapid variability of SST can be explained by variations in the heat transmission from Austral Ocean SST signals to the interior of Antarctic from one rapid event to the other. Such variations involve many further processes e.g. ocean-atmosphere heat fluxes, polar vortex position, sea-ice formation that are probably related to ice sheets volume (Rind et al., 2001; Vellinga and Wood, 2002).

AIM 2 and AIM 18, which occur during a period of very low sea levels, exhibit a particular behaviour not consistent with the same thermal bipolar seesaw pattern (Fig. 8). In fact, AIM 2 and AIM 18 warming periods are shorter than the corresponding northern stadial phases, ~ 700 yr for each instead of GS durations of 4 kyr and 5 kyr, respectively. This highlights that Antarctic warming does not systematically start with the beginning of a GS. One possibility is that AMOC is not strictly in an “off” mode during the whole GS: during both GS 3 and GS 19, the AMOC might be significantly reduced for the entire cold period in the north but could collapse just a few hundred years before the rapid Greenland event. Another possibility could be that greater southern ice volume extent (continental and sea ice) during these two particular periods would increase the isolation of Antarctica and therefore decrease the heat received by the continent from the Southern Ocean (Levermann et al., 2007).

[Title Page](#)[Abstract](#)[Introduction](#)[Conclusions](#)[References](#)[Tables](#)[Figures](#)[◀](#)[▶](#)[◀](#)[▶](#)[Back](#)[Close](#)[Full Screen / Esc](#)[Printer-friendly Version](#)[Interactive Discussion](#)

4.2.2 Sub-millennial scale variations

In Sect. 3.3, we have shown that an Antarctic counterpart exists for the sub-millennial variability recorded in Greenland. This is especially obvious for GIS 23b. When displaying the amplitude of the Antarctic warming against the duration in the Greenland cold phase (Fig. 7), we find that it is consistent with the curve representing MIS 5 events. This result highlights that even at sub-millennial scale, the bipolar seesaw model of Stocker and Johnsen (2003) is still valid.

Using an amplitude of ± 2 for T_N and a characteristic timescale of 1000 yr for the heat reservoir turned out to be the best way to describe MIS 5 rapid events. We thus apply this tuning for generating T_S curves corresponding to the sub-millennial scale structures highlighted during MIS 5 (GIS 24 and 23).

When we use a stadial duration of ~ 1250 yr with a ~ 400 yr cold phase between the precursor type peak event and the main abrupt warming, the conceptual model reproduces the same singular structure in the Antarctic counterpart as observed in the data (Fig. 9).

We then construct a time-series of T_N corresponding to GIS 24 characterised by an abrupt cooling phase lasting 200 yr (Fig. 10). We observe a plateau interrupting the regular cooling phase after AIM 24 as depicted by the temperature reconstruction of both EPICA cores. Results obtained on both events 23 and 24 emphasize the ability of the model tuned on MIS 5 to explain the sub-millennial scale variability depicted in Antarctic isotopic records.

5 Summary and perspectives

In this paper, we have presented the most recent and accurate Greenland–Antarctica common dating over the last 123 ka using the NorthGRIP and EPICA ice cores. We used new and published measurements of air isotopic composition in the NorthGRIP ice cores to compare the local amplitudes of temperature changes for GIS of MIS 5 and

Title Page

Abstract

Introduction

Conclusions

References

Tables

Figures



Back

Close

Full Screen / Esc

Printer-friendly Version

Interactive Discussion



**Millennial and
sub-millennial scale
climatic variations**

E. Capron et al.

Title Page

Abstract

Introduction

Conclusions

References

Tables

Figures



Back

Close

Full Screen / Esc

Printer-friendly Version

Interactive Discussion



MIS 3. A study of the $\delta^{18}\text{O}_{\text{ice}}$ /temperature slope at the onset of each rapid event shows a strong variability from one GIS event to another but no systematic difference between MIS 3 and MIS 5 events. For Antarctica, we have combined new and published water isotope records to present detailed temperature reconstructions of Antarctic temperature based on EPICA isotopic records.

NorthGRIP records have enabled us to depict the sub-millennial scale variability during the GIS of MIS 5. In particular, the long and warm GIS 24 is interrupted by two centennial scale cold events that present no equivalent during the glacial period but a strong analogy with the “8.2 ka” event occurring in the early Holocene (Alley et al., 1997; Leuenberger et al., 1999; Kobashi et al., 2007, Thomas et al., 2007). Going further in the description of GIS24 and the associated mechanisms requires higher resolution data.

Sub-millennial scale Greenland variability is involved in a new type of features that we have highlighted during MIS 5 (GIS 21, 23) and also during MIS 3 (GIS 11, 12, 13-14, 16). These new patterns appear as precursor-type events prior to the onset of GIS and as rebound events at the end of the GIS. In addition to the internal forcing of ice-sheets on the climatic evolution during these events, we have proposed the external influence of the summertime insolation at 65° N. In particular, we have suggested that it could help trigger the rebound event in the context of GIS (i.e. with an associated AMOC not completely “off”). Disentangling the main processes leading to these sub-millennial scale structures (ice-sheet, insolation, sea-ice, and hydrological cycle forcing) will require dedicated modelling studies. Through our results, we assume that orbital-scale variations play a role in rapid climate change but, also, the millennial-scale variability may hold clues to the long term climatic changes (i.e. Weirauch et al., 2008; Wolff et al., 2009b).

Comparing Antarctic and Greenland behaviour over the succession of AIM/DO back to MIS 5 provides a more complete description of the bipolar seesaw pattern. The “universal” linear relationship proposed in the EPICA c.-m. paper (2006) does not link the AIM amplitudes with the GS duration satisfactorily. On the contrary, the thermal bipolar

seesaw conceptual model of Stocker and Johnsen (2003) is able to represent most of the variability of the north-south relationship depicted in Greenland and Antarctic isotopic records, even at sub-millennial timescale. However, it is not able to depict the delay of Antarctic warming after the beginning of the GS during the periods associated with large ice sheets (i.e. during MIS 2 and the end of MIS 4).

To go beyond our description and the conceptual model of Stocker and Johnsen (2003), the new types of DO events identified during MIS 5 should be studied with more complex models (e.g. Ganopolski and Rahmstorf, 2001; Knutti et al., 2004). This would allow quantifying the influences of insolation, ice-sheet volume, sea-ice and hydrological cycle on sub-millennial-scale variability (precursor and rebound events). This should provide also a better understanding of the response of Antarctica to these types of events.

Acknowledgements. We are grateful to M. Crucifix, A. Govin and D. Roche for discussions and their helpful comments on the manuscript. This work was supported by ANR PICC and ANR NEEM and is a contribution to the European Project for Ice Coring in Antarctica (EPICA), a joint European Science Foundation/European Commission scientific programme, funded by the EU (EPICA-MIS) and by national contributions from Belgium, Denmark, France, Germany, Italy, the Netherlands, Norway, Sweden, Switzerland and the UK. The main logistic was provided by IPEV and PNRA (at Dome C) and AWI (at Dronning Maud Land). This work is a contribution to the North Greenland Ice Core Project (NGRIP) directed and organized by the Department of Geophysics at the Niels Bohr Institute for Astronomy, Physics and Geophysics, University of Copenhagen. It is supported by funding agencies in Denmark (SNF), Belgium (FNRS-CFB), France (IPEV and INSU/CNRS), Germany (AWI), Iceland (Rannís), Japan (MEXT), Sweden (SPRS), Switzerland (SNF) and the USA (NSF, Office of Polar Programs).



The publication of this article is financed by CNRS-INSU.

Millennial and sub-millennial scale climatic variations

E. Capron et al.

Title Page

Abstract

Introduction

Conclusions

References

Tables

Figures



Back

Close

Full Screen / Esc

Printer-friendly Version

Interactive Discussion



References

- Ahn, J. and Brook, E.: Atmospheric CO₂ and climate on millennial time scales during the last glacial period, *Science*, 322, 83–85, 2008.
- Alley, R. B., Mayewski, P. A., Sowers, T., Stuiver, M., Taylor, K. C., and Clark, P. U.: Holocene climatic instability: a prominent, widespread event 8200 years ago, *Geology*, 25, 483–486, 1997.
- Barker, S., Diz, P., Jautravers, M. J., Pike, J., Knorr, G., Hall, I. R., and Broecker, W. S.: Inter-hemispheric Atlantic seesaw response during the last deglaciation, *Nature* 457, 1097–1102, 2009.
- Bender, M., Sowers, T., Dickson, M. L., Orchardo, J., Grootes, P., Mayewski, P. A., and Meese, D. A.: Climate correlations between Greenland and Antarctica during the past 100 000 years, *Nature*, 372, 663–666, 1994.
- Bintanja, R., van de Wal, R. S. W., and Oerlemans, J.: Modelled atmospheric temperatures and global sea levels over the past million years, *Nature*, 437, 125–128, 2005.
- Blunier, T., Chappellaz, J., Schwander, J., Dällenbach, A., Stauffer, B., Stocker, T. F., Raynaud, D., Jouzel, J., Clausen, H. B., Hammer, C. U., and Johnsen, S. J.: Asynchrony of Antarctic and Greenland climate change during the last glacial period, *Nature*, 394, 739–743, 1998.
- Blunier, T. and Brook, E. J.: Timing of millennial-scale climate change in Antarctica and Greenland during the last glacial period, *Science*, 291, 109–112, 2001.
- Blunier, T., Spahni, R., Barnola, J.-M., Chappellaz, J., Loulergue, L., and Schwander, J.: Synchronization of ice core records via atmospheric gases, *Clim. Past*, 3, 325–330, 2007, <http://www.clim-past.net/3/325/2007/>.
- Bond, G., Heinrich, H., Huon, H., Broecker, W. S., Labeyrie, L., Andrews, J., McManus, J., Clasen, S., Tedesco, K., Jantschik, R., and Simet, C.: Evidence for massive discharges of icebergs into the glacial Northern Atlantic, *Nature*, 360, 245–249, 1992.
- Boyle, E. A.: Cool tropical temperatures shift the global $\delta^{18}\text{O}$ - T relationship: an explanation for the ice core $\delta^{18}\text{O}$ borehole thermometry conflict?, *Geophys. Res. Lett.*, 24, 273–276, 1997.
- Brauer, A., Allen, J. R. M., Mingram, J., Dulski, P., Wulf, S., and Huntley, B.: Evidence for interglacial chronology and environmental change from Southern Europe, *P. Natl. Acad. Sci. USA*, 104(2), 450–455, 2007.
- Braun, H., Ditlevsen, P., and Chialvo, D. R.: Solar forced Dansgaard-Oeschger events

Millennial and sub-millennial scale climatic variations

E. Capron et al.

Title Page

Abstract

Introduction

Conclusions

References

Tables

Figures



Back

Close

Full Screen / Esc

Printer-friendly Version

Interactive Discussion



and their phase relation with solar proxies, *Geophys. Res. Lett.*, 35, L06703, doi:10.1029/2008GL033414, 2008.

Broecker, W. S.: Paleocan circulation during the last deglaciation: a bipolar seesaw?, *Paleoceanography*, 13, 119–121, 1998.

5 Broecker, W. S.: Does the trigger for abrupt climate change reside in the ocean or in the atmosphere?, *Science*, 300, 1519–1522, 2003.

Broecker, W. S., Bond, G., Klas, M., Bonani, G., and Wolfli, W.: A salt oscillator in the glacial Atlantic? The concept, *Paleoceanography*, 5, 469–477, 1990.

10 Caillon, N., Severinghaus, J. P., Jouzel, J., Barnola, J.-M., Kang, J., and Lipenkov, V. Y.: Timing of atmospheric CO₂ and Antarctic temperature changes across termination III, *Science*, 299, 1728–1731, 2001.

Capron, E., Landais, A., Lemieux-Dudon, B., Schilt, A., Masson-Delmotte, V., Buiron, D., Chappellaz, J., Dahl-Jensen, D., Johnsen, S. J., Leuenberger, M., Loulergue, L., and Oerter, H.: Synchronising EDML and NorthGRIP ice cores using $\delta^{18}\text{O}$ of atmospheric oxygen ($\delta^{18}\text{O}_{\text{atm}}$) and CH₄ measurements over MIS 5 (80–123 kyr), *Quaternary Sci. Rev.*, 29, 222–234, 2010.

15 Chapman, M. R. and Shackleton, N. J.: Global ice-volume fluctuations, North Atlantic ice-rafted events, and deep-ocean circulation changes between 130 and 70 ka, *Geology*, 27, 795–798, 1999.

20 Chappellaz, J., Blunier, T., Raynaud, D., Barnola, J.-M., Schwander, J., and Stauffer, B.: Synchronous changes in atmospheric CH₄ and Greenland climate between 40 kyr and 8 kyr BP, *Nature*, 366, 443–445, 1993.

Charles, C., Rind, D., Jouzel, J., Koster, R., and Fairbanks, R.: Glacial-interglacial changes in moisture sources for Greenland: influences on the ice core record of climate, *Science*, 261, 508–511, 1994.

25 Clarke, G. K. C., Leverington, D. W., Teller, J. T., and Dyke, A. S.: Paleohydraulics of the last outburst flood from glacial Lake Agassiz and the 8200 yr BP cold event, *Quaternary Sci. Rev.*, 23, 389–407, 2004.

Cortijo, E., Duplessy, J. C., Labeyrie, L., Leclair, H., Duprat, J., and van Weering, T. C. E.: Eemian cooling in the Norwegian Sea and North Atlantic ocean preceding continental ice-sheet growth, *Nature*, 372, 446–449, 1994.

30 Crucifix, M. and Loutre, M. F.: Transient simulations over the last interglacial period (126–115 kyr BP): feedback and forcing analysis, *Clim. Dynam.*, 19, 417–433, 2002.

Cuffey, K. M. and Clow, G. D.: Temperature, accumulation and ice sheet elevation in central

Millennial and sub-millennial scale climatic variations

E. Capron et al.

Title Page

Abstract

Introduction

Conclusions

References

Tables

Figures



Back

Close

Full Screen / Esc

Printer-friendly Version

Interactive Discussion



**Millennial and
sub-millennial scale
climatic variations**

E. Capron et al.

[Title Page](#)[Abstract](#)[Introduction](#)[Conclusions](#)[References](#)[Tables](#)[Figures](#)[◀](#)[▶](#)[◀](#)[▶](#)[Back](#)[Close](#)[Full Screen / Esc](#)[Printer-friendly Version](#)[Interactive Discussion](#)

Greenland through the last deglacial transition, *J. Geophys. Res.*, 102(C12), 26383–26396, 1995.

Dahl-Jensen, D., Mosegaard, K., Gundestrup, N., Clow, G. D., Johnsen, S. J., Hansen, A. W., and Balling, N.: Past temperatures directly from the Greenland ice sheet, *Science*, 282, 268–271, 1998.

Dahl-Jensen, D., Gundestrup, N., Gorgineni, P., and Miller, H.: Basal melt at NorthGRIP modeled from borehole, ice-core and radio-echo sounder observations, *Ann. Glaciol.*, 37, 207–212, 2003.

Dansgaard, W.: Stable isotopes in precipitation, *Tellus*, 16, 436–468, 1964.

Dansgaard, W., Johnsen, S. J., Clausen, H. B., Dahl-Jensen, D., Gunderstrup, N. S., Hammer, C. U., Steffensen, J. P., Sveinbjörnsdottir, A., Jouzel, J., and Bond, G.: Evidence for general instability of past climate from a 250-kyr ice-core record, *Nature*, 364, 218–220, 1993.

Denton, G. H., Alley, R. B., Comer, G. C., and Broecker, W. S.: The role of seasonality in abrupt climate change, *Quaternary Sci. Rev.*, 24, 1159–1182, 2005.

Ditlevsen, P. D., Kristensen, M. S., and Andersen, K. K.: The recurrence time of Dansgaard-Oeschger events and limits on the possible periodic component, *J. Climate*, 18, 2594–2603, 2005.

Ditlevsen, P. D., Andersen, K. K., and Svensson, A.: The DO-climate events are probably noise induced: statistical investigation of the claimed 1470 years cycle, *Clim. Past*, 3, 129–134, 2007,
<http://www.clim-past.net/3/129/2007/>.

Eisenman, I., Bitz, C. M., and Tziperman, E.: Rain driven by receding ice sheets as a cause of past climate change, *Paleoceanography*, 24, PA4209, doi:10.1029/2009PA001778, 2009.

EPICA-community-members: One-to-one coupling of glacial climate variability in Greenland and Antarctica, *Nature*, 444, 195–198, 2006.

Eynaud, F., Turon, J.-L., Sanchez-Goni, M.-F., and Gendreau, S.: Dinoflagellate cyst evidence of “Heinrich-like events” off Portugal during the Marine Isotopic Stage 5, *Mar. Micropaleontol.*, 40, 9–21, 2000.

Fairbanks, R. G., Mortlock, R. A., Chiu, T.-C., Cao, L., Kaplan, A., Guilderson, T. P., Fairbanks, T. W., and Bloom, A. L.: Marine radiocarbon calibration curve spanning 10 000 to 50 000 years B.P. based on paired $^{230}\text{Th}/^{234}\text{U}/^{238}\text{U}$ and ^{14}C dates on pristine corals, *Quaternary Sci. Rev.*, 24, 1781–1796, 2005.

**Millennial and
sub-millennial scale
climatic variations**

E. Capron et al.

Fawcett, P. J., Agustdottir, A. M., Alley, R. B., and Shuman, C. A.: The younger dryas termination and North Atlantic deepwater formation: insights from climate model simulations and greenland ice data, *Paleoceanography*, 12, 23–38, 1996.

5 Fleitmann, D., Cheng, H., Badertscher, S., Edwards, R. L., Mudelsee, M., Göktürk, O. M., Fankhauser, A., Pickering, R., C. Raible, C. C., Matter, A., Kramers, J., and Tüysüz, O.: Timing and climatic impact of Greenland interstadials recorded in stalagmites from northern Turkey, *Geophys. Res. Lett.*, 36, L19707, doi:10.1029/2009GL040050, 2009.

10 Flückiger, J., Blunier, T., Stauffer, B., Chappellaz, M., Spahni, R., Kawamura, K., Schwander, J., Stocker, T. F., and Dahl-Jensen, D.: N₂O and CH₄ variations during the last glacial epoch: insight into global processes, *Global Biogeochem. Cy.*, 18, GB1020; doi:10.1029/2003GB002122, 2004.

Flückiger, J., Knutti, R., White, J. W. C., and Renssen, H.: Modeled seasonality of glacial abrupt climate events, *Clim. Dynam.*, 31, 633–645, 2008.

15 Friedrich, T., Timmermann, A., Timm, O., Mouchet, A., and Roche, D. M.: Orbital modulation of millennial-scale climate variability in an earth system model of intermediate complexity, *Clim. Past Discuss.*, 5, 2019–2051, 2009, <http://www.clim-past-discuss.net/5/2019/2009/>.

Gallée, H., van Ypersele, J. P., Fichefet, T., Marsiat, I., Tricot, C., and Berger, A.: Simulation of the last glacial cycle by a coupled, sectorially averaged climate-ice sheet model. Part II: response to insolation and CO variation, *J. Geophys. Res.*, 97, 15713–15740, 1992.

20 Ganopolski, A. and Rahmstorf, S.: Rapid changes of glacial climate simulated in a coupled climate model, *Nature*, 409, 153–158, 2001.

Genty, D., Blamart, D., Ouahdi, R., Gillmour, M., Baker, A., Jouzel, J., and Van-Exter, S.: Precise dating of Dansgaard Oeschger climate oscillations in Western Europe from stalagmite data, *Nature*, 421, 833–837, 2003.

25 Govin, A., Michel, E., Labeyrie, L., Waelbroeck, C., Dewilde, F., and Jansen, E.: Evidence for northward expansion of Antarctic bottom water mass in the Southern Ocean during the last glacial inception, *Paleoceanography*, 24, PA1202, 2009.

30 Grachev, A. M., Brook, E. J., Severinghaus, J. P., and Piasias, N. G.: Relative timing and variability of atmospheric methane and GISP2 oxygen isotopes between 68 and 86 ka, *Global Biogeochem. Cy.*, 23, GB2009, doi: 10.1029/2008GB003330, 2009.

Gratchev, A. M., Brook, E. J., and Severinghaus, J. P.: Abrupt changes in atmospheric methane at the MIS5b-5a transition, *Geophys. Res. Lett.*, 34, L207703, doi:10.1029/2007GL029799,

[Title Page](#)[Abstract](#)[Introduction](#)[Conclusions](#)[References](#)[Tables](#)[Figures](#)[◀](#)[▶](#)[◀](#)[▶](#)[Back](#)[Close](#)[Full Screen / Esc](#)[Printer-friendly Version](#)[Interactive Discussion](#)

2007.

GRIP-members: Climate instability during the last interglacial period recorded in the GRIP ice core, *Nature*, 364, 203–208, 1993.

Grootes, P. M., Stuiver, M., White, J. W. C., Johnsen, S. J., and Jouzel, J.: Comparison of the oxygen isotope records from the GISP2 and GRIP Greenland ice cores, *Nature*, 366, 552–554, 1993.

Grootes, P. M. and Stuiver, M.: Oxygen 18/16 variability in Greenland snow and ice with 10^{-3} - to 10^5 -year time resolution, *J. Geophys. Res.*, 102, 26455–26470, 1997.

Hendy, I. L. and Kennett, J. P.: Latest quaternary North Pacific surface-water responses imply atmosphere-driven climate instability, *Geology*, 27, 291–294, 1999.

Heusser, L. and Oppo, D. W.: Millennial- and orbital-scale climate variability in Southeastern United States and in the subtropical Atlantic during Marine Isotope Stage 5: evidence from pollen and isotopes in ODP site 1059, *Earth Planet Sc. Lett.*, 214, 483–490, 2003.

Huber, C., Leuenberger, M., Spahni, R., Flückiger, J., Schwander, J., Stocker, T. F., Johnsen, S., Landais, A., and Jouzel, J.: Isotope calibrated Greenland temperature record over Marine Isotope Stage 3 and its relation to CH_4 , *Earth Planet Sc. Lett.*, 243, 504–519, 2006.

Huybrechts, P., Rybak, O., Pattyn, F., Ruth, U., and Steinhage, D.: Ice thinning, upstream advection, and non-climatic biases for the upper 89% of the EDML ice core from a nested model of the Antarctic ice sheet, *Clim. Past*, 3, 577–589, 2007, <http://www.clim-past.net/3/577/2007/>.

Johnsen, S., Dalh-Jensen, D., Dansgaard, W., and Gundestrup, N.: Greenland palaeotemperatures derived from GRIP bore hole temperature and ice core isotope profiles, *Tellus*, 47B, 624–629, 1995.

Johnsen, S. J., Dansgaard, W., and White, J. W. C.: The origin of Arctic precipitation under present and glacial conditions, *Tellus*, 41, 452–469, 1989.

Johnsen, S. J., Clausen, H. B., Dansgaard, W., Fuhrer, K., Gundestrup, N., Hammer, C. U., Iversen, P., Jouzel, J., Stauffer, B., and Steffensen, J. P.: Irregular glacial interstadials recorded in a new Greenland ice core, *Nature*, 359, 311–313, 1992.

Johnsen, S. J., Dahl-Jensen, D., Gundestrup, N., Steffensen, J. P., Henrick, B., Clausen, H. B., Miller, H., masson-Delmotte, V., Sveinbjornsdottir, A., and White, J. W. C.: Oxygen isotope and palaeotemperature records from six Greenland ice-core stations: Camp Century, Dye-3, GRIP, GISP2, Renland and NorthGRIP, *J. Quaternary Sci.*, 16, 299–307, 2001.

Jouzel, J., Alley, R. B., Cuffey, K. M., Dansgaard, W., Grootes, P., Hoffmann, G., Johnsen, S.

CPD

6, 135–183, 2010

Millennial and sub-millennial scale climatic variations

E. Capron et al.

Title Page

Abstract

Introduction

Conclusions

References

Tables

Figures

◀

▶

◀

▶

Back

Close

Full Screen / Esc

Printer-friendly Version

Interactive Discussion



**Millennial and
sub-millennial scale
climatic variations**

E. Capron et al.

Title Page

Abstract

Introduction

Conclusions

References

Tables

Figures



Back

Close

Full Screen / Esc

Printer-friendly Version

Interactive Discussion



J., Koster, R. D., Peel, D., Shuman, C. A., Stievenard, M., Stuiver, M., and White, J.: Validity of the temperature reconstruction from ice cores, *J. Geophys. Res.*, 102, 26 471–26 487, 1997.

Jouzel, J.: Calibrating the isotopic paleothermometer, *Science*, 286, 910–911, 1999.

Jouzel, J., Vimeux, F., Caillon, N., Delaygue, G., Hoffmann, G., Masson-Delmotte, V., and Parrenin, F.: Magnitude of the isotope/temperature scaling for interpretation of central Antarctic ice cores, *J. Geophys. Res.*, 108, 1029–1046, 2003.

Jouzel, J., Masson-Delmotte, V., Cattani, O., Dreyfus, G., Falourd, S., Hoffmann, G., Minster, B., Nouet, J., Barnola, J.-M., Fisher, H., Gallet, J.-C., Johnsen, S., Leuenberger, M., Loulergue, L., Luethi, D., Oerter, H., Parrenin, F., Raisbeck, G., Raynaud, D., Schilt, A., Schwander, J., Selmo, J., Souchez, R., Spahni, R., Stauffer, B., Steffensen, J.-P., Stenni, B., Stocker, T. F., Tison, J.-L., Werner, M., and Wolff, E. W.: Orbital and millennial Antarctic climate variability over the past 800 000 years, *Science*, 317, 793–796, 2007.

Kageyama, M., Mignot, J., Swingedouw, D., Marzin, C., Alkama, R., and Marti, O.: Glacial climate sensitivity to different states of the Atlantic Meridional Overturning Circulation: results from the IPSL model, *Clim. Past*, 5, 551–570, 2009, <http://www.clim-past.net/5/551/2009/>.

Khodri, M., Leclainche, Y., Ramstein, G., Braconnot, P., Marti, O., and Cortijo, E.: Simulating the amplification of orbital forcing by ocean feedbacks in the last glaciation, *Nature*, 410, 570–574, 2001.

Khodri, M., Ramstein, G., de Noblet-Ducoudre, N., and Kageyama, M.: Sensitivity of the Northern extratropics hydrological cycle to the changing insolation forcing at the 126 and 115 kyr BP, *Clim. Dynam.*, 21, 273–287, 2003.

Kiefer, T., Sarnthein, M., Erlenkeuser, H., Grootes, P. M., and Roberts, A. P.: North Pacific response to millennial-scale in the ocean circulation in the last 60 ka, *Paleoceanography*, 16(2), 179–189, 2001.

Knutti, R., Flückiger, J., Stocker, T. F., and Timmermann, A.: Strong hemispheric coupling of glacial climate through freshwater discharge and ocean circulation, *Nature*, 430, 851–856, 2004.

Kobashi, T., Severinghaus, J. P., Brook, E. J., Barnola, J. M., and Grachev, A. M.: Precise timing and characterization of abrupt climate change 8200 years ago from air trapped in Polar ice, *Quaternary Sci. Rev.*, 26, 1212–1222, 2007.

Krinner, G., Genthon, C., and Jouzel, J.: GCM analysis of local influences on ice core δ signals,

**Millennial and
sub-millennial scale
climatic variations**

E. Capron et al.

Title Page

Abstract

Introduction

Conclusions

References

Tables

Figures

◀

▶

◀

▶

Back

Close

Full Screen / Esc

Printer-friendly Version

Interactive Discussion



Geophys. Res. Lett., 24, 2825–2828, 1997.

Landais, A., Barnola, J. M., Masson-Delmotte, V., Jouzel, J., Chappellaz, J., Caillon, N., Huber, C., Leuenberger, M., and Johnsen, S. J.: A continuous record of temperature evolution over a sequence of Dansgaard-Oeschger events during Marine Isotopic Stage 4 (76 to 62 kyr BP), Geophys. Res. Lett., 31, L22211.1-L22211.4, doi:10.1029/2004GL021193, 2004a.

Landais, A., Caillon, N., Goujon, C., Grachev, A. M., Barnola, J. M., Chappellaz, J., Jouzel, J., Masson-Delmotte, V., and Leuenberger, M.: Quantification of rapid temperature change during DO event 12 and phasing with methane inferred from air isotopic measurements, Earth Planet. Sc. Lett., 225, 221–232, 2004b.

Landais, A., Caillon, N., Severinghaus, J., Barnola, J.-M., Goujon, C., Jouzel, J., and Masson-Delmotte, V.: Isotopic measurements of air trapped in ice to quantify temperature changes, C. R. Geosci., 336, 963–970, 2004c.

Landais, A., Masson-Delmotte, V., Jouzel, J., Raynaud, D., Johnsen, S., Huber, C., Leuenberger, M., Schwander, J., and Minster, B.: The glacial inception as recorded in the North-GRIP Greenland ice core: timing, structure and associated abrupt temperature changes, Clim. Dynam., 26, 273–284, 2006.

Landais, A., Dreyfus, D., Capron, E., Sanchez-Goni, M. F., Desprat, S., Jouzel, J., Hoffmann, G., and Johnsen, S.: What drive orbital- and millennial-scale variations of the $\delta^{18}\text{O}$ of atmospheric oxygen?, Quaternary Sci. Rev., 29, 235–246, 2010.

Lang, C., Leuenberger, M., Schwander, J., and Johnsen, S.: 16 °C rapid temperature variation in central Greenland 70 000 years ago, Science, 286, 934–937, 1999.

Laskar, J., Robutel, P., Joutel, F., Gastineau, M., Correia, A. C. M., and Levrard, B.: A long-term numerical solution for the insolation quantities of the Earth, Astron. Astrophys., 428, 261–285, 2004.

Leuenberger, M. C., Lang, C., and Schwander, J.: $\delta^{15}\text{N}$ measurements as a calibration tool for the paleothermometer and gas–ice age differences: a case study for the 8200 BP event on GRIP ice, J. Geophys. Res.-Atmos., 104, 22163–22170, 1999.

Levermann, A., Schewe, J., and Montoya, M.: Lack of bipolar seesaw in response to Southern Ocean wind reduction, Geophys. Res. Lett., 34, L12711, doi:10.1029/2007GL0302552007.

Li, C., Battisti, D. S., Schrag, D. P., and Tziperman, E.: Abrupt climate shifts in Greenland due to displacements of the sea ice edge, Geophys. Res. Lett., L19702, doi:10.1029/2005GL023492, 32, 2005.

Liu, Z., Otto-Bliesner, B. L., He, F., Brady, E. C., Tomas, R., Clark, P. U., Carlson, A. E., Lynch-

**Millennial and
sub-millennial scale
climatic variations**

E. Capron et al.

Title Page

Abstract

Introduction

Conclusions

References

Tables

Figures

◀

▶

◀

▶

Back

Close

Full Screen / Esc

Printer-friendly Version

Interactive Discussion



- Stieglitz, J., Curry, W., Brook, E., Erickson, D., Jacob, R., Kutzbach, J., and Cheng, J.: Transient simulation of last deglaciation with a new mechanism for Bølling-Allerød warming, *Science*, 325, 310–314, 2009.
- Lorius, C. and Merlivat, L.: Distribution of mean surface stable isotope values in East Antarctica. Observed changes with depth in a coastal area, in: *Isotopes and Impurities in Snow and Ice*, edited by: IAHS Publication, IAHS, Vienna, 125–137, 1977.
- Loulergue, L., Schilt, A., Spahni, R., Masson-Delmotte, V., Blunier, T., Lemieux, B., Barnola, J.-M., Raynaud, D., Stocker, T. F., and Chappellaz, J.: Orbital and millennial-scale features of atmospheric CH₄ over the past 800 000 years, *Nature*, 453, 383–386, 2008.
- Luethi, D., Le Floch, M., Bereiter, B., Blunier, T., Barnola, J.-M., Siegenthaler, U., Raynaud, D., Jouzel, J., Fischer, H., Kawamura, K., and Stocker, T. F.: High-resolution carbon dioxide concentration record 650 000–800 000 years before present, *Nature*, 453, 379–382, 2008.
- MacAyeal, D. R.: Binge/purge oscillations of the Laurentide ice sheet as a cause of the North Atlantic's Heinrich events, *Paleoceanography*, 8, 775–784, 1993.
- Mariotti, A.: Atmospheric nitrogen as a reliable stable standard for ¹⁵N abundance measurements, *Nature*, 303, 685–687, 1983.
- Masson-Delmotte, V., Stenni, B., and Jouzel, J.: Common millennial scale variability of Antarctic and southern ocean temperatures during the past 5000 years reconstructed from EPICA Dome C ice core, *Holocene*, 14, 145–151, 2004.
- Masson-Delmotte, V., Jouzel, J., Landais, A., Stievenard, M., Johnsen, S. J., White, J. W. C., Sveinbjornsdottir, A., and Fuhrer, K.: Deuterium excess reveals millennial and orbital scale fluctuations of Greenland moisture origin, *Science*, 309, 118–121, 2005.
- Masson-Delmotte, V., Hou, S., Ekaykin, A., Jouzel, J., Aristarain, A., Bernardo, R. T., Bromwich, D., Cattani, O., Delmotte, M., Falourd, S., Frezzotti, M., Gallée, H., Genoni, L., Isaksson, E., Landais, A., Helsen, M. M., Hoffmann, G., Lopez, J., Morgan, V., Motoyama, H., Noone, D., Oerter, H., Petit, J. R., Royer, A., Uemura, R., Schmidt, G. A., Schlosser, E., Simões, J. C., Steig, E. J., Stenni, B., Stievenard, M., van den Broeke, M. R., van de Wal, R. S. W., van de Berg, W. J., Vimeux, F., and White, J. W. C.: A review of Antarctic surface snow isotopic composition: observations, atmospheric circulation and isotopic modelling, *J. Climate*, 21, 3359–3387, 2008.
- McManus, J. F., Bond, G. C., Broecker, W. S., Johnsen, S. J., Labeyrie, L., and Higgins, S.: High-resolution climatic records from the North Atlantic during the last interglacial, *Nature*, 371, 326–329, 1994.

**Millennial and
sub-millennial scale
climatic variations**

E. Capron et al.

Title Page

Abstract

Introduction

Conclusions

References

Tables

Figures

◀

▶

◀

▶

Back

Close

Full Screen / Esc

Printer-friendly Version

Interactive Discussion



- McManus, J. F., Oppo, D. W., and Cullen, J.-L.: A 0.5-million-year record of the millennial-scale climate variability in the North Atlantic, *Science*, 283, 971–975, 1999.
- Meyer, H., Schönicke, L., Wand, U., Hubberten, H.-W., and Friedrichsen, H.: Isotope studies of hydrogen and oxygen in ground ice? Experiences with the equilibration technique, *Isot. Environ. Health S.*, 36, 133–149, 2000.
- Meyer, M. C., Spötl, C., and Magini, A.: The demise of the last interglacial recorded in isotopically speleothems from the Alps, *Quaternary Sci. Rev.*, 27, 476–496, 2008.
- Monnin, E., Indermühle, A., Dällenbach, A., Flückiger, J., Stauffer, B., Stocker, T. F., Raynaud, D., and Barnola, J.-M.: Atmospheric CO₂ concentrations over the last glacial termination, *Science*, 291, 112–114, 2001.
- NorthGRIP-community-members: High-resolution record of Northern Hemisphere climate extending into the last interglacial period, *Nature*, 431, 147–151, 2004.
- Oerter, H., Graf, W., Meyer, H., and Wilhelms, F.: The EPICA ice core from Dronning Maud Land: first results from stable-isotope measurements, *Ann. Glaciol.*, 39, 307–312, 2004.
- Oppo, D. W., Lloyd, D., Keigwin, L. D., and McManus, J. F.: Persistent suborbital climate variability in Marine Isotope Stage 5 and Termination II, *Paleoceanography*, 16, 280–292, 2001.
- Otto-Bliesner, B. L. and Brady, E. C.: The sensitivity of the climate response to the magnitude and location of freshwater forcing: last glacial maximum experiments, *Quaternary Sci. Rev.*, 29, 56–73, 2010.
- Parrenin, F., Barnola, J.-M., Beer, J., Blunier, T., Castellano, E., Chappellaz, J., Dreyfus, G., Fischer, H., Fujita, S., Jouzel, J., Kawamura, K., Lemieux-Dudon, B., Loulergue, L., Masson-Delmotte, V., Narcisi, B., Petit, J.-R., Raisbeck, G., Raynaud, D., Ruth, U., Schwander, J., Severi, M., Spahni, R., Steffensen, J. P., Svensson, A., Udisti, R., Waelbroeck, C., and Wolff, E.: The EDC3 chronology for the EPICA Dome C ice core, *Clim. Past*, 3, 485–497, 2007a, <http://www.clim-past.net/3/485/2007/>.
- Parrenin, F., Dreyfus, G., Durand, G., Fujita, S., Gagliardini, O., Gillet, F., Jouzel, J., Kawamura, K., Lhomme, N., Masson-Delmotte, V., Ritz, C., Schwander, J., Shoji, H., Uemura, R., Watanabe, O., and Yoshida, N.: 1-D-ice flow modelling at EPICA Dome C and Dome Fuji, East Antarctica, *Clim. Past*, 3, 243–259, 2007b, <http://www.clim-past.net/3/243/2007/>.
- Peterson, L. C., Haug, G. H., Hughen, K. A., and Röhl, U.: Rapid changes in the hydrologic cycle of the Tropical Atlantic during the last glacial, *Science*, 290, 1947–1951, 2000.

**Millennial and
sub-millennial scale
climatic variations**

E. Capron et al.

Title Page

Abstract

Introduction

Conclusions

References

Tables

Figures

◀

▶

◀

▶

Back

Close

Full Screen / Esc

Printer-friendly Version

Interactive Discussion

Petit, J. R., Jouzel, J., Raynaud, D., Barkov, N. I., Barnola, J. M., Basile, I., Bender, M., Chappel-
laz, J., Davis, M., Delaygue, G., Delmotte, M., Kotlyakov, V. M., Legrand, M., Lipenkov, V. Y.,
Lorius, C., Pepin, L., Ritz, C., Saltzman, E., and Stievenard, M.: Climate and atmospheric
history of the past 420,000 years from the Vostok ice core, Antarctica, *Nature*, 399, 429–436,
1999.

Rahmstorf, S.: Timing of abrupt climate change: a precise clock, *Geophys. Res. Lett.*, 30,
30(10), 1050, doi:10.1029/2003GL017115, 2003.

Rind, D., Demenocal, P., Russell, G. L., Sheth, S., Collins, D., Schmidt, G. A., and Teller, J.:
Effects of glacial meltwater in the GISS Coupled Atmosphere-Ocean Model: Part I: North
Atlantic Deep Water response, *J. Geophys. Res.*, 106, 27335–27354, 2001.

Rousseau, D. D., Kukla, G., and McManus, J.: What is what in the ice and the ocean?, *Quater-
nary Sci. Rev.*, 25, 2025–2030, 2006.

Ruth, U., Barnola, J.-M., Beer, J., Bigler, M., Blunier, T., Castellano, E., Fischer, H., Fundel, F.,
Huybrechts, P., Kaufmann, P., Kipfstuhl, S., Lambrecht, A., Morganti, A., Oerter, H., Par-
renin, F., Rybak, O., Severi, M., Udisti, R., Wilhelms, F., and Wolff, E.: “EDML1”: a chronol-
ogy for the EPICA deep ice core from Dronning Maud Land, Antarctica, over the last 150 000
years, *Clim. Past*, 3, 475–484, 2007,
<http://www.clim-past.net/3/475/2007/>.

Sanchez Goñi, M. F., Turon, J.-L., Eynault, F., and Gendreau, S.: European climatic response
to millennial-scale changes in the atmosphere-ocean system during the last glacial period,
Quaternary Res., 54, 394–403, 2000.

Sanchez Goñi, M. F., Cacho, I., Turon, J.-L., Guiot, J., Sierro, F. J., Peyrouquet, J.-P., and
Shackleton, N. J.: Synchronicity between marine and terrestrial responses to millennial scale
climatic variability during the last glacial period in the Mediterranean region, *Clim. Dynam.*,
19, 95–105, 2002.

Schulz, M., Paul, A., and Timmermann, A.: Relaxation oscillators in concert: a framework for
climate change at millennial timescales during the late Pleistocene, *Geophys. Res. Lett.*,
29(24), 2193, doi:10.1029/2002GL016144, 29, 2002a.

Schulz, M.: On the 1470-year pacing of Dansgaard-Oeschger warm events, *Paleoceanography*,
4.1–4.10, 17, 2002b.

Severi, M., Becagli, S., Castellano, E., Morganti, A., Traversi, R., Udisti, R., Ruth, U., Fischer, H.,
Huybrechts, P., Wolff, E., Parrenin, F., Kaufmann, P., Lambert, F., and Steffensen, J. P.: Syn-
chronisation of the EDML and EDC ice cores for the last 52 kyr by volcanic signature match-

ing, *Clim. Past*, 3, 367–374, 2007,
<http://www.clim-past.net/3/367/2007/>.

Severinghaus, J. P., Sowers, T., Brook, E. J., Alley, R. B., and Bender, M. L.: Timing of abrupt climate change at the end of the Younger Dryas interval from thermally fractionated gases in Polar ice, *Nature*, 391, 141–146, 1998.

Severinghaus, J. P. and Brook, E. J.: Abrupt climate change at the end of the last glacial period inferred from trapped air in polar ice, *Science*, 286, 930–934, 1999.

Shackleton, N. J. and Pisias, N. G.: Atmospheric carbon dioxide, orbital forcing, and climate, *Geoph. Monog. Series*, 32, 412–417, 1985.

Shackleton, N. J.: Oxygen isotopes, ice volume and sea level, *Quaternary Sci. Rev.*, 6, 183–190, 1987.

Shackleton, N. J., Sanchez-Göñi, M. F., Pailler, D., and Lancelot, Y.: Marine isotope substage 5e and the Eemian interglacial, *Global Planet. Change*, 36, 151–155, 2003.

Siddall, M., Thomas, F., Stocker, T., Blunier, T., Spahni, R., Schwander, J., Barnola, J.-M., and Chappellaz, J.: Marine Isotope Stage (MIS) 8 millennial variability stratigraphically identical to MIS 3, *Paleoceanography*, 22, PA1208, doi:10.1029/2006PA001345, 2007.

Sime, L. C., Wolff, E. W., Oliver, K. I. C., and Tindall, J. C.: Evidence for warmer interglacials, *Nature*, 462, 342–345, 2009.

Sprovieri, R., Di Stefano, E., Alessandro Incarbona, A., and Oppo, D. W.: Suborbital climate variability during Marine Isotopic Stage 5 in the central Mediterranean basin: evidence from calcareous plankton record, *Quaternary Sci. Rev.*, 25, 2332–2342, 2006.

Steffensen, J. P., Andersen, K. K., Bigler, M., Clausen, H. B., Dahl-Jensen, D., Fischer, H., Goto-Azuma, K., Hansson, M., Johnsen, S. J., Jouzel, J., Masson-Delmotte, V., Popp, T., Rasmussen, S. O., Röthlisberger, R., Ruth, U., Stauffer, B., Siggaard-Andersen, M.-L., Sveinbjörnsdóttir, A. E., Svensson, A., and White, J. W. C.: High-resolution Greenland ice core data show abrupt climate change happens in few years, *Science*, 321, 680–683, 2008.

Stenni, B., Masson-Delmotte, V., Johnsen, S., Jouzel, J., Longinelli, A., Monnin, E., Röthlisberger, R., and Selmo, E.: An oceanic cold reversal during the last deglaciation, *Science*, 293, 2074–2077, 2001.

Stenni, B., Selmo, E., Masson-Delmotte, V., Oerter, H., Meyer, H., Rothlisberger, R., Jouzel, J., Cattani, O., Falourd, S., Fischer, H., Hoffmann, G., Lacumin, P., Johnsen, S. J., and Minster, B.: The deuterium excess records of EPICA Dome C and Dronning Maud Land ice cores (East Antarctica), *Quaternary Sci. Rev.*, 29, 146–159, 2010.

CPD

6, 135–183, 2010

Millennial and sub-millennial scale climatic variations

E. Capron et al.

Title Page

Abstract

Introduction

Conclusions

References

Tables

Figures

◀

▶

◀

▶

Back

Close

Full Screen / Esc

Printer-friendly Version

Interactive Discussion



**Millennial and
sub-millennial scale
climatic variations**

E. Capron et al.

[Title Page](#)[Abstract](#)[Introduction](#)[Conclusions](#)[References](#)[Tables](#)[Figures](#)[Back](#)[Close](#)[Full Screen / Esc](#)[Printer-friendly Version](#)[Interactive Discussion](#)

- Stocker, T. F., Wright, D. G., and Mysak, L. A.: A zonally averaged, coupled ocean-atmosphere model for paleoclimate studies, *J. Climate*, 5, 773–797, 1992.
- Stocker, T. F. and Johnsen, S. J.: A minimum thermodynamic model for the bipolar seesaw, *Paleoceanography*, 18, 1087, 2003.
- 5 Svensson, A., Andersen, K. K., Bigler, M., Clausen, H. B., Dahl-Jensen, D., Davies, S. M., Johnsen, S. J., Muscheler, R., Parrenin, F., Rasmussen, S. O., Röthlisberger, R., Seierstad, I., Steffensen, J. P., and Vinther, B. M.: A 60 000 year Greenland stratigraphic ice core chronology, *Clim. Past*, 4, 47–57, 2008, <http://www.clim-past.net/4/47/2008/>.
- 10 Swingedouw, D., Fichet, T., Goosse, H., and Loutre, M. F.: Impact of transient freshwater releases in the Southern Ocean on the AMOC and climate, *Clim. Dynam.*, 33, 365–381, 2009.
- Thomas, E. R., Wolff, E. W., Mulvaney, R., Steffensen, J. P., Johnsen, S. J., Arrowsmith, C., White, J. W. C., Vaughn, B., and Popp, T.: The 8.2 ka event from Greenland ice cores, *Quaternary Sci. Rev.*, 26, 70–81, 2007.
- 15 van Krevelend, S. A., Sarnthein, M., Erlenkeuser, H., Grootes, P., Jung, S., Nadeau, M. J., Pflaumann, U., and Voelker, A. H. L.: Potential links between surging ice sheets, circulation changes and the Dansgaard-Oeschger cycles in the Irminger Sea, 60–18 kyr, *Paleoceanography*, 15, 425–442, 2000.
- 20 Vellinga, M. and Wood, R. A.: Global climatic impacts of a collapse of the Atlantic thermohaline circulation, *Climatic Change*, 54, 251–267, 2002.
- Vimeux, F., Cuffey, K., and Jouzel, J.: New insights into Southern Hemisphere temperature changes from Vostok ice cores using deuterium excess correction over the last 420 000 years, *Earth Planet Sc. Lett.*, 203, 829–843, 2002.
- 25 Vinther, B. M., Buchardt, S. L., Clausen, H. B., Dahl-Jensen, D., Johnsen, S. J., Fisher, D. A., Koerner, R. M., Raynaud, D., Lipenkov, V., Andersen, K. K., Blunier, T., Rasmussen, S. O., Steffensen, J. P., and Svensson, A. M.: Holocene thinning of the Greenland ice sheet, *Nature*, 461, 385–388, 2009.
- Voelker, A. H. L.: Global distribution of centennial-scale records for Marine Isotope Stage (MIS) 3: a database, *Quaternary Sci. Rev.*, 21, 1185–1212, 2002.
- 30 von Grafenstein, U., Erlenkeuser, H., Müller, J., Jouzel, J., and Johnsen, S. J.: The cold event 8200 years ago documented in oxygen isotope records of precipitation in Europe and Greenland, *Clim. Dynam.*, 14, 73–81, 1998.

**Millennial and
sub-millennial scale
climatic variations**

E. Capron et al.

- Waelbroeck, C., Labeyrie, L., Michel, E., Duplessy, J. C., McManus, J. F., Lambeck, K., Balbon, E., and Labracherie, M.: Sea-level and deep water temperature changes derived from benthic foraminifera isotopic records, *Quaternary Sci. Rev.*, 21, 295–305, 2002.
- 5 Wang, Y., Cheng, H., Edwards, R. L., Kong, X., Shao, X., Chen, S., Wu, J., Jiang, X., Wang, X., and An, Z.: Millennial- and orbital-scale changes in the East Asian monsoon over the past 224 000 years, *Nature*, 451, 1090–1093, 2008.
- Wang, Y. J., Cheng, H., Edwards, R. L., An, Z. S., Wu, J. Y., Shen, C.-C., and Dorale, J. A.: A high-resolution absolute-dated late Pleistocene monsoon record from Hulu Cave, China, *Science*, 94, 2345–2348, 2001.
- 10 Wang, Z. and Mysak, L. A.: Glacial abrupt climate changes and Dansgaard-Oeschger oscillations in a coupled climate model, *Paleoceanography*, 21, PA2001, doi:10.1029/2005PA001238, 21, 2006.
- Weirauch, D., Billups, K., and Martin, P.: Evolution of millennial-scale climate variability during the mid-Pleistocene, *Paleoceanography*, PA3216, doi:10.1029/2007PA001584, 23, 2008.
- 15 Wolff, E. W., Chappellaz, J., Blunier, T., Rasmussen, S. O., and Svensson, A.: Millennial-scale variability during the last glacial: the ice core record, *Quaternary Sci. Rev.*, doi:10.1016/j.quascirev.2009.10.013 2009a.
- Wolff, E., Fischer, H., and Rothlisberger, R.: Glacial terminations as southern warmings without northern control, *Nat. Geosci.*, 2, 206–209, 2009b.
- 20 Wunsch, C.: Abrupt climate change: an alternative view, *Quaternary Res.*, 65, 191–203, 2006.

[Title Page](#)[Abstract](#)[Introduction](#)[Conclusions](#)[References](#)[Tables](#)[Figures](#)[◀](#)[▶](#)[◀](#)[▶](#)[Back](#)[Close](#)[Full Screen / Esc](#)[Printer-friendly Version](#)[Interactive Discussion](#)

Millennial and sub-millennial scale climatic variations

E. Capron et al.

Table 1. Uncertainties on MIS 5 DO events duration associated with the new EDML-NorthGRIP common timescale over MIS 5 (Capron et al., 2010). The uncertainty determination is based on the comparison of DO duration inferred from the EDML-NorthGRIP timescale with their duration on other timescales (marine sediment cores: MD95-2042, Shackelton et al., 2004 and NEAP18K, Chapman and Shackelton, 2002; Sanbao Cave speleothem record, Wang et al., 2008; lake record from Monticchio, Brauer et al., 2007).

	DO duration on each chronology (yr) ^a					Mean σ (yr) ^b	Event duration uncertainty (%) ^c
	(1) EDML-NGRIP	(2) MD95-2042	(3) NEAP-18K	(4) Sambaio Cave	(5) Monticchio		
DO25	5530	3950	2990	3970	2610	1520	28
DO24	4850	4130	4940	5150	4820	200	4
DO23	12570	11190	11530	13900	9460	1210	10
DO22	5870	6300	4940	6750	5340	490	8
DO21	9350	6460	9700	7360		1230	13

^a DO duration on each chronology: (1) EDML-NorthGRIP timescale, (2) MD95-2042 timescale, (3) NEAP18K timescale, (4) Sambaio Cave timescale, (5) Lago di Monticchio timescale.

^b For each rapid event, we calculate the standard deviation between the event duration on the EDML-NorthGRIP chronology and its duration on each other 4 timescales (not shown here) and deduce a mean standard deviation, σ , from the 4 standard deviation calculations.

^c The uncertainty of each event duration is given as a percentage of error deduced from values depicted in ^b on the DO duration deduced from EDML-NorthGRIP timescale (column 1).

Title Page

Abstract

Introduction

Conclusions

References

Tables

Figures

◀

▶

◀

▶

Back

Close

Full Screen / Esc

Printer-friendly Version

Interactive Discussion



Table 2. North-South rapid events recorded in NorthGRIP and EPICA ice cores.

DO	NG $\Delta\delta^{18}\text{O}_{\text{ice}}$ (‰) ^a	NG ΔT (°C) ^b	Reference	NorthGRIP α (‰/°C) ^c	GS Δt (yr) ^d	AIM	EDML ΔT (°C) ^e	Reference
2	3.9				4100±100 (1)	2	2±0.4	This study
3	5.5				800±150 (1)	3	0.6±0.2	EPICA c.-m., 2006
4	4.9				1600±250 (1)	4	1.8±0.2	EPICA c.-m., 2006
5	4.2				900±150(1)	5	1.1± 0.2	EPICA c.-m., 2006
6	4.2				1000±150 (1)	6	1.2±0.3	EPICA c.-m., 2006
7	4.2				1300±250 (1)	7	1.9±0.3	EPICA c.-m., 2006
8	4.7	11 (+3;−6)	Huber et al., 2006	0.61	1800±150 (1)	8	2.7±0.3	EPICA c.-m., 2006
9	2.6	9 (+3;−6)	Huber et al., 2006	0.47	800±150 (1)	9	0.8±0.3	EPICA c.-m., 2006
10	4	11.5 (+3;−6)	Huber et al., 2006	0.33	2000± 250 (1)	10	1.4±0.2	EPICA c.-m., 2006
11	5.4	15 (+3;−6)	Huber et al., 2006	0.36	1100±150 (1)	11	1.5±0.4	This study
12	5.6	12.5 (+3;−6)	Huber et al., 2006	0.52	1600±150 (1)	12	2.4±0.4	EPICA c.-m., 2006
13	2.9	8 (+3;−6)	Huber et al., 2006	0.54	#	13		
14	4.9	12±2.5	Huber et al., 2006	0.47	#	14		
15	4	10 (+3;−6)	Huber et al., 2006	0.58	#	15		
16	3.9	9 (+3;−6)	Huber et al., 2006	0.59	#	16		
17	4	12 (+3;−6)	Huber et al., 2006	0.54	#	17		
18	4.5	11±2.5	Landais et al., 2004a	0.40	5200±100 (2)	18	1.7±0.4	This study
19	6.7	16±2.5	Landais et al., 2004a	0.43	1600±150 (2)	19	2.1±0.4	This study
20	6	11±2.5	Landais et al., 2004a	0.55	1200±150 (2)	20	1.5±0.4	This study
21	4.2	12±2.5	This study	0.4	3600±300 (3)	21	4.2±0.4	This study
22	2	4.5±2.5	This study		#	22	*	This study
23	3.3	10±2.5	Landais et al., 2006	0.36	1400±200 (3)	23	2.4±0.4	This study
23a	3.8				300±60 (3)	23a	1±0.4	This study
24	5	16±2.5	Landais et al., 2006	0.31	1700±100 (3)	24	3±0.4	This study
25	1.9					25		

^a NorthGRIP $\delta^{18}\text{O}_{\text{ice}}$ amplitude ($\Delta\delta^{18}\text{O}_{\text{ice}}$) at the onset of abrupt events (NorthGRIP c.-m., 2004).

^b Accompanying warming amplitude (ΔT) estimated from $\delta^{15}\text{N}$ data with associated uncertainty (Huber et al., 2006; Landais et al., 2006; this study).

^c Spatial slope deduced at the onset of each rapid event as $\alpha = \Delta\delta^{18}\text{O}_{\text{ice}} / \Delta T$. Note that a $\pm 2.5^\circ\text{C}$ uncertainty on temperature change is translated to an error of ~ 0.2 in the calculation of α .

^d GS durations are given to the nearest century (1) on the GICC05 age scale to 50 ka (Blunier et al., 2007; Svensson et al., 2008), (2) on ss09sea age scale between 60 and 75 ka (NorthGRIP c.-m., 2004) and (3) on the EDML-NorthGRIP synchronised timescale between 75 and 123 ka (Capron et al., 2010). GS duration is defined by the interval between the midpoint of the stepwise temperature change at the start and end of a stadial. The errors associated with stadial duration are estimated by using different splines through the data that affect the width of the DO transitions and are linked to visual determination of maxima and minima during transitions. No estimate of GS is given where the beginning of the GS is hard to pinpoint due to the particular structure of events and the corresponding events are labeled with #.

^e AIM warming amplitudes are given for the EDML ice core based on the temperature reconstruction of Stenni et al. (2010). AIM 22 is damped after d-excess corrections and labeled as * (see Stenni et al. (2010) for details). The amplitude is determined following EPICA c.-m. (2006) from the Antarctic $\delta^{18}\text{O}_{\text{ice}}$ maximum to the preceding minimum of each event. Uncertainties on MIS 3 AIM amplitudes are determined in EPICA c.-m. (2006). For AIM events during MIS 2, MIS 4 and MIS 5, we consider that an error bar of $\pm 0.4^\circ\text{C}$ encompasses the uncertainty on the determination of the warming amplitude by using different splines through the data.

Millennial and sub-millennial scale climatic variations

E. Capron et al.

Title Page

Abstract

Introduction

Conclusions

References

Tables

Figures

◀

▶

◀

▶

Back

Close

Full Screen / Esc

Printer-friendly Version

Interactive Discussion



Millennial and sub-millennial scale climatic variations

E. Capron et al.

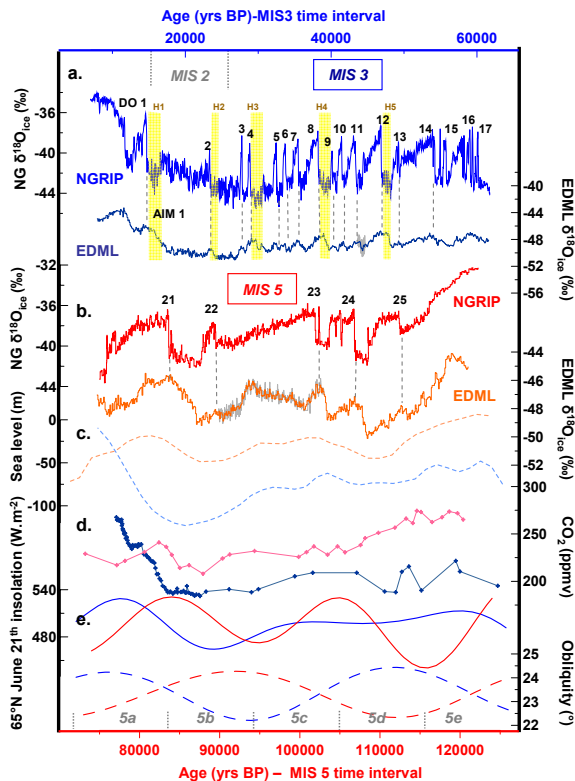


Fig. 1. Comparison of some climatic parameters over MIS 3 and MIS 5. **(a)** MIS 3 NorthGRIP $\delta^{18}\text{O}_{\text{ice}}$ (light blue curve, NorthGRIP c.-m., 2004) and EDML $\delta^{18}\text{O}_{\text{ice}}$ (dark blue curve, EPICA c.-m., 2006; grey curve, this study). **(b)** MIS 5 NorthGRIP $\delta^{18}\text{O}_{\text{ice}}$ (red curve, NorthGRIP c.-m., 2004) and EDML $\delta^{18}\text{O}_{\text{ice}}$ (orange curve, EPICA c.-m., 2006; grey curve, this study). **(c)** MIS 3 (dotted light blue curve) and MIS 5 (dotted orange curve) sea level variations (Waelbroeck et al., 2002). **(d)** MIS 3 (dark blue curve) and MIS 5 (pink curve) CO_2 concentration. CO_2 records are from EDC (Monnin et al., 2001) and Vostok ice cores (Petit et al., 1999) and compiled by Luethi et al., 2008. **(e)** MIS 3 and MIS 5 orbital contexts (65°N summer insolation and obliquity, Laskar et al., 2004). Note that new $\delta^{18}\text{O}_{\text{ice}}$ measurements were performed over AIM events 11 and 23 (grey curve) at Alfred Wegener Institute (Germany) with a depth resolution of 0.05 m, using the CO_2 (H_2)/water equilibration technique (Meyer et al., 2000).

Title Page

Abstract

Introduction

Conclusions

References

Tables

Figures

◀

▶

◀

▶

Back

Close

Full Screen / Esc

Printer-friendly Version

Interactive Discussion



Millennial and sub-millennial scale climatic variations

E. Capron et al.

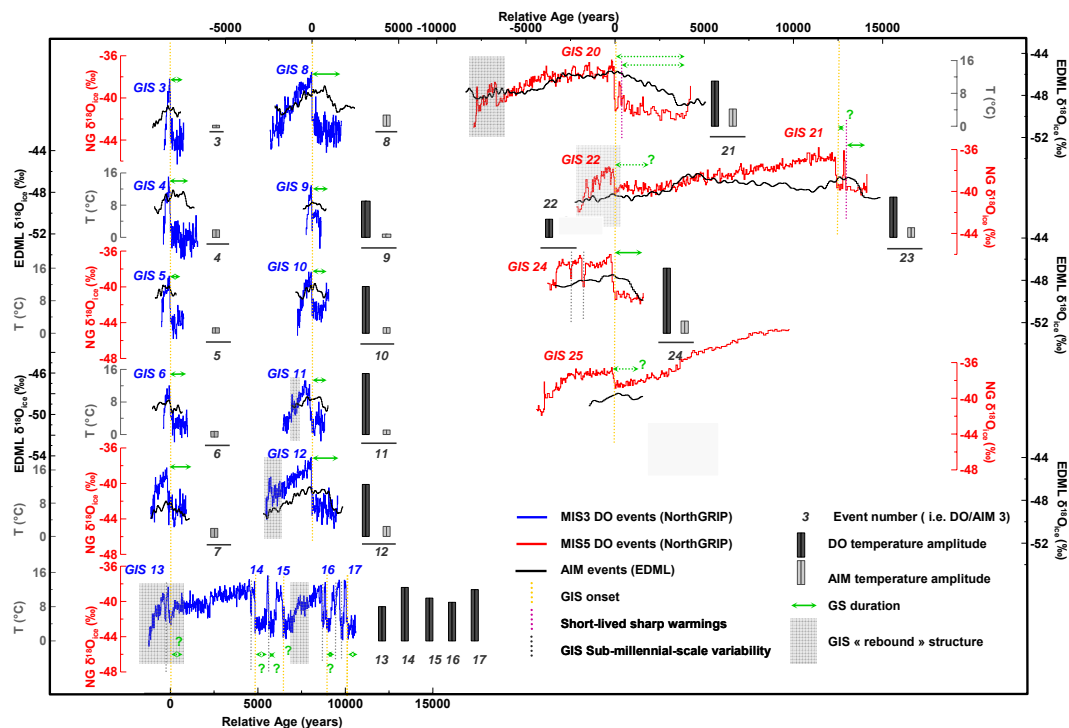


Fig. 2. Synthesis of millennial and sub-millennial scale climatic variability during MIS 3 (blue curve) and MIS 5 (red curve) recorded in NorthGRIP $\delta^{18}\text{O}_{\text{ice}}$ (NorthGRIP c.-m., 20004) on a relative age centred on the onset of Greenland rapid events. AIM events recorded in EDML $\delta^{18}\text{O}_{\text{ice}}$ are superimposed (EPICA c.-m., 2006; grey curve). Numbers indicate GIS events and corresponding AIM events. Vertical dotted bars mark onsets of GIS (yellow) and precursor-type peak events (purple), sub-millennial scale variability over sequence of events 13–17 and GIS 24 (grey). Shaded grey bands indicate rebound-type events. Horizontal grey arrows materialise GS duration. Bars represent amplitudes of local temperature increase at the onset of GIS events based on $\delta^{15}\text{N}$ measurements (dark bars; Huber et al., 2006; Landais et al. 2006; this study) and AIM warming amplitudes (grey bars).

Title Page

Abstract

Introduction

Conclusions

References

Tables

Figures



Back

Close

Full Screen / Esc

Printer-friendly Version

Interactive Discussion



Millennial and sub-millennial scale climatic variations

E. Capron et al.

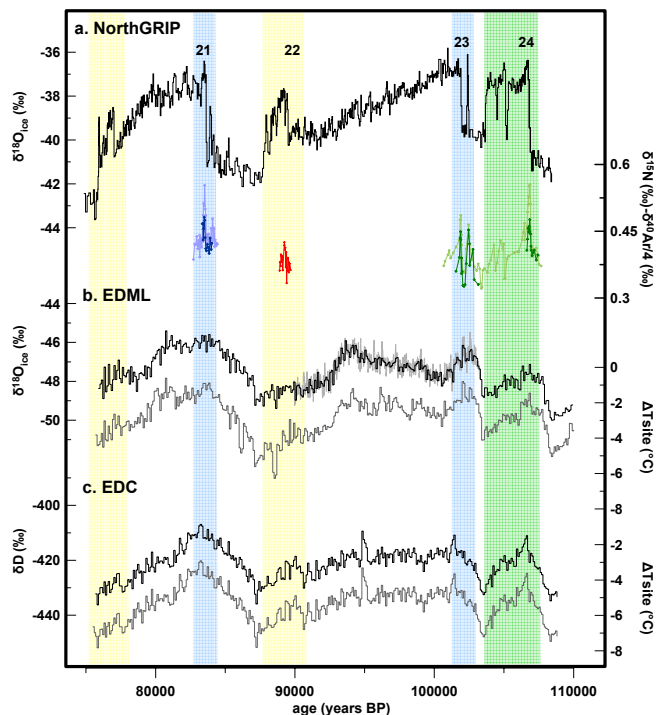


Fig. 3. Greenland-Antarctic isotopic records between 75 and 109 ka. **(a)** NorthGRIP $\delta^{18}\text{O}_{\text{ice}}$ records (black curve, NorthGRIP c.-m., 2004), $\delta^{15}\text{N}$ measurements at the onset of GIS 21 (light blue curve, Capron et al., 2010), 22 (red curve, this study), 23 and 24 (light green curve, Landais et al., 2006) and $\delta^{40}\text{Ar}$ measurements at the onset of GIS 21 (dark blue curve, this study), 23 and 24 (dark green curve, Landais et al., 2006). **(b)** EDML $\delta^{18}\text{O}_{\text{ice}}$ plot of i) bag sample data filtered on 100 yr time step (black curve; EPICA c.-m., 2006) and ii) high-resolution data (a 50 yr smoothing is performed on the 10 yr time step data, light grey curve, this study) and T_{site} reconstruction from Stenni et al. (2010, a 700 yr smoothing is performed on the 100 yr time step data, dark grey curve). **(c)** EDC $\delta^{18}\text{O}_{\text{ice}}$ plot of bag sample data filtered on 100 yr time step (black curve; Jouzel et al., 2007) and T_{site} reconstruction from Stenni et al. (2010; a 700 yr smoothing is performed on the 100 yr time step data, dark grey curve). Shaded bands mark the sub-millennial scale variability over MIS 5 GIS and their counterparts in Antarctica (Rebound-type events, yellow; Precursor-type events, blue; GIS 24, green).

Title Page

Abstract

Introduction

Conclusions

References

Tables

Figures

◀

▶

◀

▶

Back

Close

Full Screen / Esc

Printer-friendly Version

Interactive Discussion



Millennial and sub-millennial scale climatic variations

E. Capron et al.

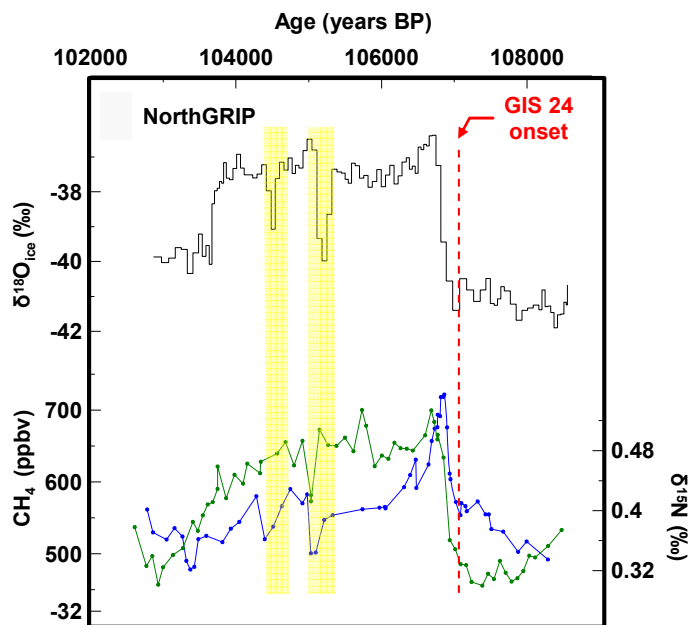


Fig. 4. GIS 24 recorded in NorthGRIP $\delta^{18}\text{O}_{\text{ice}}$ (black, NorthGRIP c.-m., 2004), $\delta^{15}\text{N}$ (blue; Landais et al., 2006) and CH_4 (green, Capron et al., 2010). Red dotted line marks the synchronous onset of GIS 24 recorded in both ice and gas phases. Yellow shaded bands highlight abrupt coolings which interrupt the interstadial phase.

Title Page

Abstract

Introduction

Conclusions

References

Tables

Figures

◀

▶

◀

▶

Back

Close

Full Screen / Esc

Printer-friendly Version

Interactive Discussion



Millennial and sub-millennial scale climatic variations

E. Capron et al.

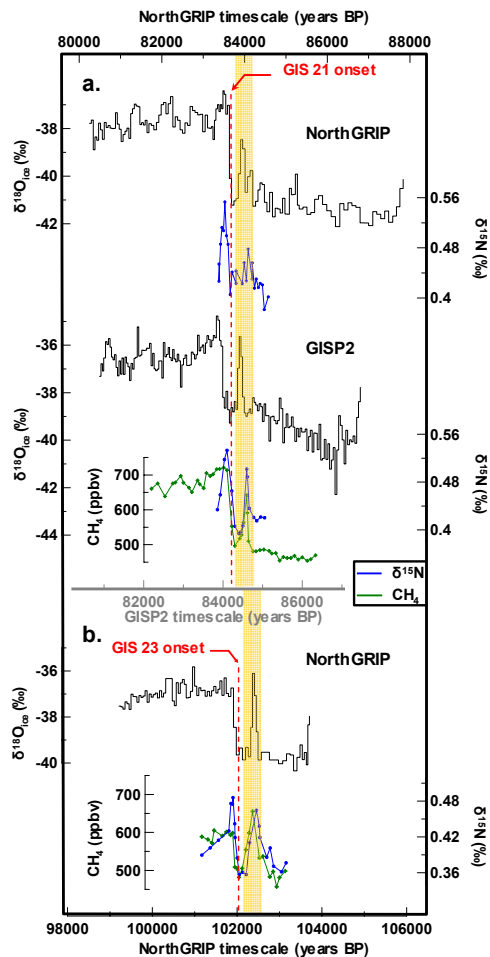


Fig. 5. (a) Short-lived sharp warming preceding GIS 21 recorded in NorthGRIP $\delta^{18}\text{O}_{\text{ice}}$ (NorthGRIP c.-m., 2004) and $\delta^{15}\text{N}$ (this study) and in GISP2 $\delta^{18}\text{O}_{\text{ice}}$ (Grootes and Stuiver, 1993), $\delta^{15}\text{N}$ and CH_4 (Gratchev et al., 2007). (b) Short-lived sharp warming preceding GIS 23 recorded in NorthGRIP $\delta^{18}\text{O}_{\text{ice}}$ (NorthGRIP c.-m., 2004) CH_4 (Capron et al., 2010) and $\delta^{15}\text{N}$ (this study).

Title Page

Abstract

Introduction

Conclusions

References

Tables

Figures

◀

▶

◀

▶

Back

Close

Full Screen / Esc

Printer-friendly Version

Interactive Discussion

Millennial and sub-millennial scale climatic variations

E. Capron et al.

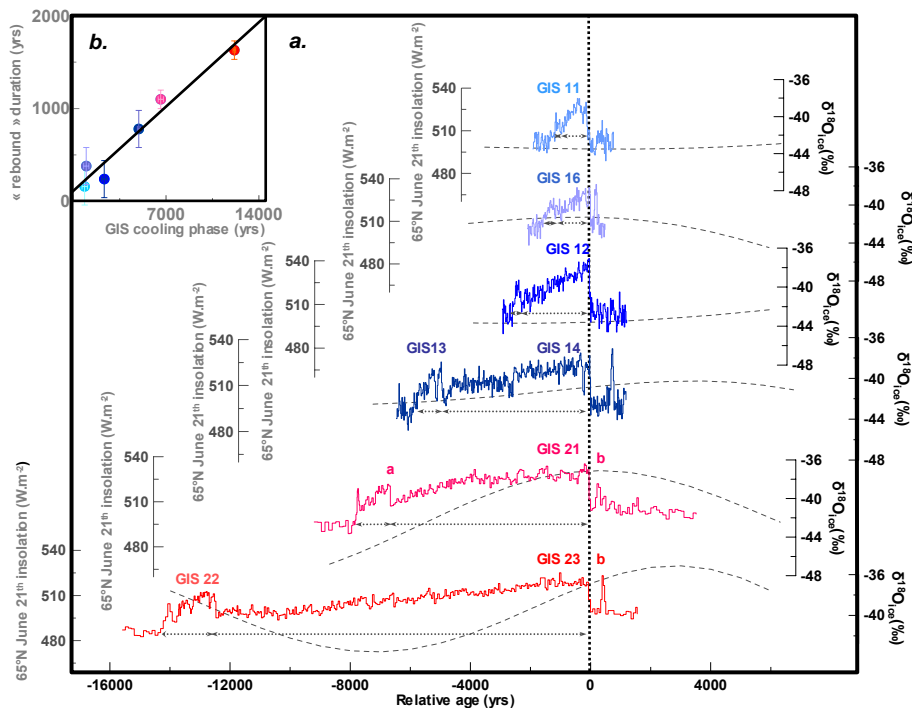


Fig. 6. (a) Sub-millennial scale climatic variability characterised by GIS preceding by precursor-type peak events and a rebound structure after GIS regular cooling phase (NorthGRIP c.-m., 2004). 65° N insolation is superimposed to NorthGRIP isotopic records (Laskar et al., 2004). Dotted grey arrows evidenced the gradual GIS cooling phase followed by the abrupt warming depicted as a “rebound” event. (b) Linear relationship between GIS cooling phase duration and associated duration of the rebound with associated uncertainties ($R^2=0.95$).

Title Page

Abstract

Introduction

Conclusions

References

Tables

Figures

◀

▶

◀

▶

Back

Close

Full Screen / Esc

Printer-friendly Version

Interactive Discussion



Millennial and sub-millennial scale climatic variations

E. Capron et al.

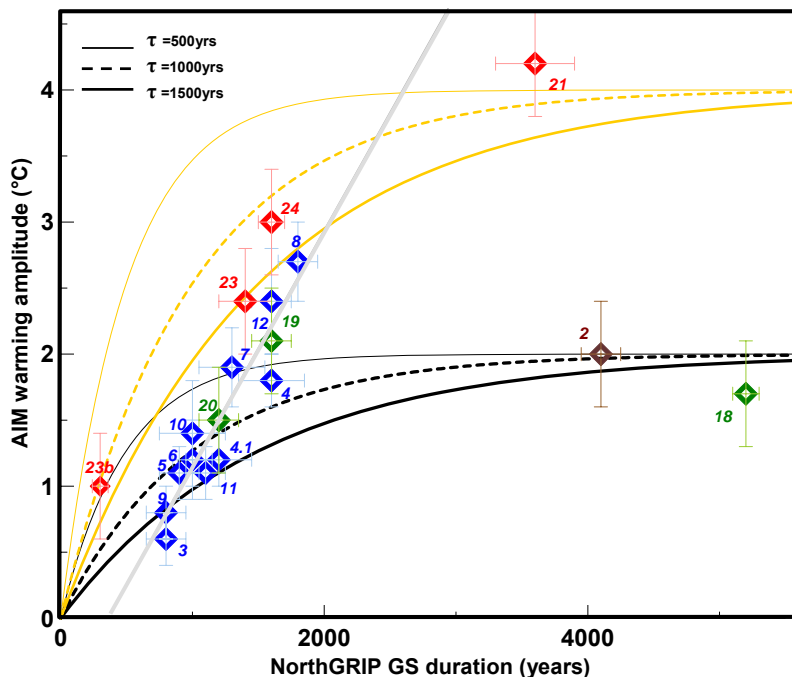


Fig. 7. Greenland stadial durations versus AIM warming amplitude over the last glacial period (MIS 5: red diamond, MIS 3: blue diamond, MIS 4: green diamond, MIS 2: brown diamond). Associated uncertainties are determined following EPICA c.-m. (2006). Numbers indicate the corresponding AIM and DO events. Linear relationship for MIS 3 events established in EPICA c.-m. (2006; light grey line). Evolutions of the relationship between Greenland stadial durations and AIM warming amplitudes inferred from the conceptual model for a thermal bipolar seesaw (Stocker and Johnsen, 2003; Eq. 1) depending on i) different characteristic timescales (500 yr, thin curve; 1000 yr, dotted thick curve; 1500 yr, thick curve) and ii) different values for T_N ($-1/+1$ amplitude, black curves; $-2/+2$ amplitude; yellow curves).

Title Page

Abstract

Introduction

Conclusions

References

Tables

Figures

◀

▶

◀

▶

Back

Close

Full Screen / Esc

Printer-friendly Version

Interactive Discussion



Millennial and sub-millennial scale climatic variations

E. Capron et al.

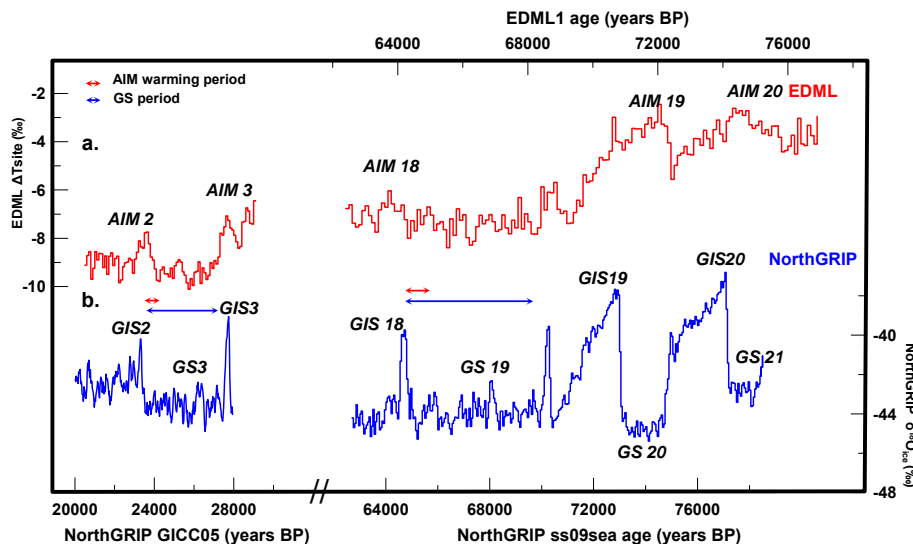


Fig. 8. (a) EDML1 ΔT_{site} (Stenni et al., 2010) over AIM 2 and the sequence of events from AIM 18 to AIM 20. All are presented on the EDML1 timescale (Ruth et al., 2007). (b) NorthGRIP $\delta^{18}O_{ice}$ over 20–28 ka: GICC05 timescale (Svensson et al., 2008); over 63–79 ka: ss09sea glaciological timescale (NorthGRIP c.-m., 2004). Red Arrows represent warming durations of AIM 2 and AIM 18 and blue arrows represent GS 3 and GS 20 durations.

Title Page

Abstract

Introduction

Conclusions

References

Tables

Figures

◀

▶

◀

▶

Back

Close

Full Screen / Esc

Printer-friendly Version

Interactive Discussion



Millennial and sub-millennial scale climatic variations

E. Capron et al.

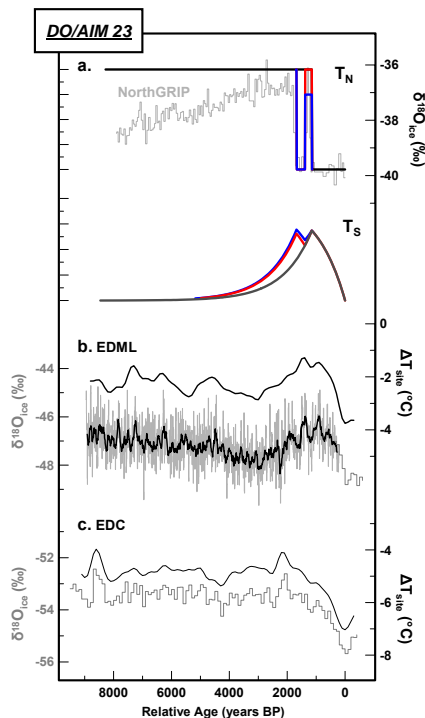


Fig. 9. (a) North-south time-series generated by the conceptual thermal bipolar seesaw model (Stocker and Johnsen, 2003) for GIS 23 superimposed NorthGRIP $\delta^{18}\text{O}_{\text{ice}}$ data (light grey curve). Two configurations (blue and red) are used to simulate response of the Southern Hemisphere (T_s) to the northern perturbation (T_N). (b) EDML high-resolution data (a 50 yr smoothing is performed on the 10 yr time step data, light grey curve, this study) and T_{site} reconstruction from Stenni et al. (2010, a 700 yr smoothing is performed on the 100 yr time step data, dark grey curve). (c) EDC $\delta^{18}\text{O}_{\text{ice}}$ (grey step curve) and temperature reconstruction (dark grey curve; Stenni et al., 2010).

Title Page

Abstract

Introduction

Conclusions

References

Tables

Figures

◀

▶

◀

▶

Back

Close

Full Screen / Esc

Printer-friendly Version

Interactive Discussion



Millennial and sub-millennial scale climatic variations

E. Capron et al.

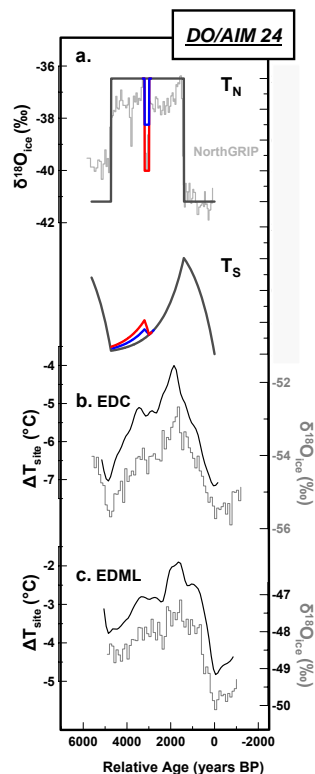


Fig. 10. (a) North-south time-series generated by the conceptual thermal bipolar seesaw model (Stocker and Johnsen, 2003) for GIS 24. For the north, grey line represented NorthGRIP $\delta^{18}\text{O}_{\text{ice}}$ data. Two configurations (blue and red curves) are used to simulate response of the Southern Hemisphere (T_{S}) to the northern perturbation (T_{N}). (b) EDC $\delta^{18}\text{O}_{\text{ice}}$ (Jouzel et al., 2007) and temperature reconstruction (Stenni et al., 2010). (c) EDML $\delta^{18}\text{O}_{\text{ice}}$ (EPICA c.-m., 2006) and temperature reconstruction (Stenni et al., 2010).

Title Page

Abstract

Introduction

Conclusions

References

Tables

Figures

◀

▶

◀

▶

Back

Close

Full Screen / Esc

Printer-friendly Version

Interactive Discussion

